Gallium Complexation, Stability, and Bioconjugation of 1,4,7-Triazacyclononane Derived Chelators with Azaheterocyclic Arms

Schmidtke, Alexander ; Läppchen, Tilman ; Weinmann, Christian ; Bier-Schorr, Lorenz ; Keller, Manfred ; Kiefer, Yvonne ; Holland, Jason P ; Bartholomä, Mark D

Abstract: We have recently introduced a 1,4,7-triazacyclononane (TACN) based chelating system with additional five-membered azaheterocyclic substituents for complexation of radioactive Cu2+ ions. In this work, we investigated the complexation properties of these novel chelators with Ga3+. In labeling experiments, we could show that the penta- and hexadentate imidazole derivatives NODIA-Me 4 and NOTI-Me 1 can be labeled with 68Ga in specific activities up to 30 MBq nmol–1, while the corresponding thiazole derivative NOTThia 2 did not label satisfactorily under identical conditions. NMR studies on the Ga complexes of 1 and the model compound NODIA-Me-NH-Me 5 revealed formation of rigid 1:1 chelates with a slow macrocyclic interconversion and inert Ga–N bonds to the methylimidazole residues on the NMR time scale. The TACN-derived bifunctional chelator NODIA-Me was furthermore conjugated to a prostate-specific membrane antigen (PSMA) targeting moiety to give the corresponding bioconjugate NODIA-Me-PSMA 7. Serum stability and ligand challenge experiments of 68Ga-7 confirmed formation of a stable complex for up to 4 h. The remaining coordination site of five-coordinate Ga complexes was found to be occupied by monodentate ligands including hydroxide and chloride anions depending on the conditions. According to density functional theory calculations, coordination of monodentate ligands as well as of the amide group for the bioconjugated ligand are energetically plausible. Finally, the labeled bioconjugate 68Ga-7 exhibited rapid renal clearance in biodistribution studies performed by small animal PET imaging with no indication of transchelation/demetalation in vivo. Altogether, our results provide strong evidence for a stable Ga complexation of our novel TACN-based chelators bearing imidazole arms. Despite the formation of two complexes incorporating different monodentate ligands in vitro, the imidazole type ligands show promise as chelating agents for the future development of gallium based radiopharmaceuticals.

DOI: https://doi.org/10.1021/acs.inorgchem.7b01129

Gallium complexation, stability and bioconjugation of TACN derived chelators with azaheterocyclic arms

Alexander Schmidtke[1], Tilman Läppchen[1,3], Christian Weinmann[1], Lorenz Bier-Schorr[1], Manfred Keller[2], Yvonne Kiefer[1], Jason P. Holland[1,4], and Mark D. Bartholomä[1,*]

[1] Department of Nuclear Medicine, Medical Center – University of Freiburg, Faculty of Medicine, University of Freiburg, Hugstetterstrasse 55, D-79106, Freiburg, Germany

[2] Department of Chemistry, University of Freiburg, D-79104, Freiburg, Germany

[3] Department of Nuclear Medicine, Inselspital, Bern University Hospital and University of Bern, Freiburgstrasse, CH-3010 Bern, Switzerland

[4] Department of Chemistry, University of Zurich, Winterthurerstrasse 190, CH-8057, Zurich, Switzerland

*** Corresponding Author:**

Dr. Mark D. Bartholomä

Tel: +49-(761)-270-39600

Fax: +49-(761)-270-39300

E-mail: mark.bartholomae@uniklinik-freiburg.de

Key words: Gallium-68, prostate-specific membrane antigen (PSMA), positron-emission tomography, chelator.

Abstract

We have recently introduced a 1,4,7-triazacyclononane (TACN) based chelating system with additional five-membered azaheterocyclic substituents for complexation of radioactive Cu^{2+} ions. In this work, we investigated the complexation properties of these novel chelators with Ga^{3+}. In labelling experiments, we could show that the penta- and hexadentate imidazole derivatives NODIA-Me **4** and NOTI-Me **1** can be labelled with ^{68}Ga in specific activities up to ~30 MBq $nmol^{-1}$, while the corresponding thiazole derivative NOTThia **2** did not label satisfactorily under identical conditions. NMR studies on the Ga complexes of **1** and the model compound NODIA-Me-NH-Me **5** revealed formation of rigid 1:1 chelates with a slow macrocyclic interconversion and inert Ga-N bonds to the methylimidazole residues on the NMR time scale. The TACN-derived bifunctional chelator NODIA-Me was furthermore conjugated to a prostate-specific membrane antigen (PSMA) targeting moiety to give the corresponding bioconjugate NODIA-Me-PSMA **7**. Serum stability and ligand challenge experiments of ^{68}Ga-**7** confirmed formation of a stable complex for up to 4h. The remaining coordination site of five-coordinate Ga complexes was found to be occupied by monodentate ligands including hydroxide and chloride anions depending on the conditions. According to density functional theory (DFT) calculations, coordination of monodentate ligands are energetically plausible. Finally, the labelled bioconjugate ^{68}Ga-**7** exhibited rapid renal clearance in biodistribution studies performed by small animal PET imaging with no indication of transchelation/demetallation *in vivo*. Altogether, our results provide strong evidence for a stable Ga complexation of our novel TACN-based chelators bearing imidazole arms. Despite the formation of two complexes with different monodentate ligands *in vitro*, the imidazole type ligands show promise as chelating agents for the future development of gallium based radiopharmaceuticals.

Introduction

In recent years, the positron-emitting radionuclide ^{68}Ga has been used intensively in both preclinical and clinical research.[1-11] Interest in ^{68}Ga originates from its ready availability from commercial ^{68}Ge/^{68}Ga generator systems, which allow cost-effective, widespread use of ^{68}Ga-based radiopharmaceuticals at clinical centers that do not have access to local cyclotron facilities. The parent radionuclide ^{68}Ge has a half-life of 271 days and typical commercial generators can be used for ≥1 year. Gallium-68 has a half-life of 67.7 min and decays primarily by positron emission (β^+: 89%, E_{β^+max} = 1899 keV). Its half-life provides a close match with the pharmacokinetics of many peptides and other small molecules owing to a fast blood clearance as well as rapid diffusion and target localization. The availability of ^{68}Ge/^{68}Ga generator systems and optimal decay properties of ^{68}Ga have spurred the development of ^{68}Ga-based radiopharmaceuticals in recent years.[12] The most prominent example for the clinical success of ^{68}Ga-labelled radiopharmaceuticals is the family of ^{68}Ga-labelled somatostatin analogs which include DOTATATE (1,4,7,10-tetraazacyclododecane-*N*,*N*′,*N*″,*N*‴-tetraacetic acid-d-Phe(1),Tyr(3)-octreotate) for PET imaging of neuroendocrine tumors.[13-16] More recently, two urea-based radiopharmaceuticals ^{68}Ga-HBED-CC-PSMA (also known as DKFZ-PSMA-11)[17-24] and ^{68}Ga-PSMA Imaging & Therapy[25-27] targeting the prostate specific membrane antigen (PSMA) have shown great promise in clinical PET imaging of prostate cancer and metastases.

Labelling biomolecules with radiometals for imaging and/or therapy generally requires the use of a bifunctional chelator (BFC). The BFC is designed to bind the radiometal at one terminus and contains at least one functional group as a second terminus for covalent linkage to a targeting vector of interest. Introduction of a BFC into a biomolecule can induce adverse effects on the radiolabelling chemistry, biological binding properties, and on the pharmacokinetics of the

radiotracer *in vivo*. The most commonly used BFC for ^{68}Ga is the ligand DOTA (1,4,7,10-tetraazacyclododecane-1,4,7,10-tetraacetic acid) given in Scheme 1.[28] Its popularity originated from its versatility in coordinating a wide range of medically important radiometals, e.g. ^{177}Lu-DOTATATE for somatostatin receptor radiotherapy. However, for DOTA conventional or microwave heating is required in order to obtain adequate radiochemical yields (RCYs) and specific activities.[29-33] Another well-established family of BFCs for ^{68}Ga is based on the macrocycle TACN (1,4,7-triazacyclononane) such as the ligands NOTA (1,4,7-triazacyclononane-1,4,7-triacetic acid) and NODAGA (1,4,7-triazacyclononane-*N*-glutamic acid-*N'*,*N''*-diacetic acid) shown in Scheme 1. These TACN based chelators have been radiolabelled efficiently at low temperatures and even at ambient temperature.[34-37] Other ligands, reported more recently, that label under ambient conditions are the ligands TRAP (1,4,7-triazacyclononane-1,4,7-tris[methyl(2-carboxyethyl)phosphinic acid)[38-40] and PCTA (3,6,9,15-tetraazabicyclo[9.3.1]pentadeca-1(15),11,13-triene-3,6,9-triacetic acid).[41-44] While most of the ligands used for ^{68}Ga complexation are based on macrocycles, the acyclic ligand HBED-CC (*N*,*N'*-bis[2-hydroxy-5-(carboxyethyl)benzyl]ethylenediamine-*N*,*N'*-diacetic acid) in Scheme 1 has recently received increased attention as the complexing unit of the radiopharmaceutical ^{68}Ga-HBED-CC-PSMA.[17-24]

We have recently introduced a novel chelating system based on the macrocycle TACN with pendant five-membered azaheterocycles, which was originally designed for stable complexation of radioactive Cu^{2+} ions.[45] These ligands radiolabel efficiently with ^{64}Cu under mild conditions over a wide pH range in high specific activities. The corresponding ^{64}Cu complexes displayed high inertness/stability *in vitro*. While many ligands for Ga^{3+} complexation that utilize different O- and N-donor groups have been described, to the best of our knowledge, macrocyclic

ligands bearing azaheterocyclic pendant substituents with aromatic N-donors have not been reported. Interestingly, there are only a few reports in the literature on the Ga chemistry of five-membered azaheterocycles in aqueous media.[46-47] In the present work, we therefore sought to explore the potential of novel TACN derived chelators with azaheterocyclic residues for $^{nat./68}Ga^{3+}$ complexation.

Materials and Methods

Chemicals and solvents of the highest grade commercially available were purchased from Sigma-Aldrich (Schnelldorf, Germany) and TCI Europe (Zwijndrecht, Belgium), and used as received. ^{1}H and ^{13}C NMR spectra were measured in MeOD or D_2O at room temperature using a Bruker Avance III HD 500MHz NMR spectrometer (Rheinstetten, Germany). Chemical shifts are given in parts per million (ppm) and are reported relative to tetramethylsilane (TMS) or 4,4-dimethyl-4-silapentane-1-sulfonic acid (DSS), respectively. Coupling constants are reported in hertz (Hz). The multiplicity of the NMR signals is described as follows: s = singlet, d = doublet, t = triplet, q = quartet, m = multiplet. Low resolution electrospray ionisation mass spectrometry (LR-ESI(+)-MS) was performed on a PerkinElmer Flexar SQ 300 MS Detector (Rodgau, Germany). High resolution mass spectrometry (HR-ESI(+)-MS) was performed on a Thermo Scientific Exactive mass spectrometer (Langenselbold, Germany). Automated GMP conform radiolabelling with $^{68}GaCl_3$ was accomplished using a synthesis module (Pharmtracer, Eckert & Ziegler, Berlin, Germany) with an IGG100 generator (Eckert & Ziegler). High performance liquid chromatography (HPLC) was conducted on an Agilent (Waldbronn, Germany) 1260 Infinity System equipped with an Agilent 1200 DAD UV detector (UV detection at 220 nm) and a Raytest Ramona radiation detector (Straubenhardt, Germany) in series. A Phenomenex (Aschaffenburg, Germany) Jupiter Proteo (250 x 4.60 mm) column was used for analytical HPLC. The solvent system was A = H_2O (0.1% TFA) and B = acetonitrile (0.1% TFA). The gradient was 0-1 min at 5% B, 1-12 min from 5% to 50% B at a flow rate of 1 mL min^{-1}. Semi-preparative HPLC was performed on a Knauer Smartline 1000 HPLC system (Berlin, Germany) in combination with a Macherey Nagel VP 250/21 Nucleosil 120-5 C18 column (Düren, Germany). Conditions A were 0-40 min from 5% to 60% B at a flow rate of 12 mL min^{-1}. Conditions B were 0-10 min from 5% to 45% B, 10-13 min from

45% to 95% B at a flow rate of 12 mL min^{-1}. Conditions C were 0-5 min from 5% to 10% B, 10-20 min from 10% to 20% B at a flow rate of 12 mL min^{-1}. Samples were lyophilized by using a Christ Alpha 1-2 LD plus lyophilizer (Osterode, Germany). All instruments measuring radioactivity were calibrated and maintained in accordance with previously reported routine quality-control procedures.[48] Radioactivity measurements were made by using an Activimeter ISOMED 2010 (Nuklear-Medizintechnik, Dresden, Germany). For accurate quantification of radioactivity, experimental samples were counted for 1 min on a calibrated Perkin Elmer (Waltham, MA) 2480 Automatic Wizard Gamma Counter by using a dynamic energy window of 400–600 keV for ^{68}Ga (511 keV emission). Phosphorimaging was performed using a Cyclone Plus (Perkin Elmer).

Synthesis

The precursor Glu-CO-Lys(Ahx)-$(tBu)_3$ ester was purchased from ABX (Radeberg, Germany). The ligand NOTA (1,4,7-triazacyclononane-1,4,7-triacetic acid) was obtained from Chematech (Dijon, France). NOTI-Me **1** (1,4,7-tris((1-methyl-1*H*-imidazol-2-yl)methyl)-1,4,7-triazonane), NOTThia **2** (1,4,7-tris(thiazol-2-ylmethyl)-1,4,7-triazonane) and the disubstituted TACN derivative NODI-Me **3** (1,4-bis[(1-methyl-1*H*-imidazol-2-yl)methyl]-1,4,7-triazonane) were prepared as previously described.[45]

*NODIA-Me (2-(4,7-bis((1-methyl-1H-imidazol-2-yl)methyl)-1,4,7-triazonan-1-yl)acetic acid) (**4**)*

NODI-Me **3** (100 mg, 0.32 mmol) was mixed with glyoxylic acid monohydrate (58 mg, 0.63 mmol) in 10 mL 1,2-dichloroethane followed by the addition of sodium triacetoxyborohydride (400 mg, 1.89 mmol). The suspension was allowed to stir for 16 h at room temperature. The

reaction mixture was concentrated to dryness by rotary evaporation and the residue redissolved in 5 mL water (0.1% TFA) and further purified by semi-preparative RP-HPLC to give NODIA-Me **4** as colorless solid after lyophilization (106 mg, 0.28 mmol, 90%). ^{1}H NMR (MeOD): δ = 2.77 (m, 4H), 3.08 (m, 4H), 3.45 (m, 4H), 3.89 (s, 6H), 4.14 (s, 2H), 4.24 (s, 4H), 7.52 (d, *J* = 2.0, 2H), 7.53 (d, *J* = 2.0, 2H) ppm; ^{13}C NMR (MeOD): δ = 35.3, 48.1, 49.6, 51.6, 54.2, 58.5, 120.3, 125.5, 145.0, 170.1 ppm. HR-ESI(+)-MS calcd m/z for $C_{18}H_{29}N_7O_2$ $(M+H)^+$: 376.2461, found: 376.2457. RP-HPLC (semi-preparative, conditions B): t_R = 6.5 min; RP-HPLC (analytical, UV: 220 nm): t_R = 3:11 min.

*NODIA-Me-NH-Me (*2-(4,7-bis((1-methyl-1*H*-imidazol-2-yl)methyl)-1,4,7-triazonan-1-yl)-*N*-methylacetamide) ***(5)***

NODIA-Me **4** (50 mg, 0.13 mmol) was reacted with methylamine hydrochloride (18 mg, 0.26 mmol) in the presence of HATU (1-[bis(dimethylamino)methylene]-1*H*-1,2,3-triazolo[4,5-*b*]pyridinium 3-oxid hexafluorophosphate) (101 mg, 0.26 mmol) and DIPEA (*N,N*-diisopropylethylamine) (138 mg, 185 µL, 1.06 mmol) in 5 mL DMF for 4 h. The solvent was removed by azeotropic rotary evaporation using toluene (3 x 10 mL). The residue was redissolved in 5 mL of water:acetonitrile 0.1% TFA (50:50) and purified by semi-preparative RP-HPLC (conditions C). Fractions containing the product were combined followed by rotary evaporation of acetonitrile under vacuum. The remaining aqueous phase was then lyophilized to give NODIA-Me-NH-Me **5** as colorless solid (44 mg, 0.11 mmol, 86%). ^{1}H NMR (MeOD): δ = 2.77 (m, 4H), 2.86 (s, 3H), 3.07 (m, 4H), 3.42 (m, 4H), 3.91 (s, 6H), 4.18 (s, 2H), 4.23 (s, 4H), 7.56 (d, *J* = 2.0, 2H), 7.57 (d, *J* = 2.0, 2H) ppm; ^{13}C NMR (MeOD): δ = 26.8, 35.4, 47.7, 49.4, 51.3, 54.0, 58.2,

120.3, 125.6, 145.0, 166.9 ppm. HR-ESI(+)-MS calcd m/z for $C_{19}H_{32}N_8O$ $(M+H)^+$: 389.2772, found: 389.2769. RP-HPLC (semi-preparative, conditions C): t_R = 13 min.

*^{nat}Ga NOTI-Me (Ga-**1**)*

NOTI-Me **1** (20 mg, 0.05 mmol) and gallium nitrate hydrate (12 mg, 0.05 mmol) each dissolved in 500 µL water were combined and heated at 95 °C for 30 min. The ^{nat}Ga complex Ga-**1** was obtained as colorless powder after lyophilization (32 mg, 0.05 mmol, 99%). ^{1}H NMR (D_2O, pD < 2): δ = 2.77 (m, 3H), 3.47 (m, 6H), 3.65 (m, 3H), 3.72 (s, 9H), 4.34 (d, J = 17.2, 3H), 4.81 (d, J = 17.2, 3H), 6.48 (d, J = 1.8, 3H), 7.37 (d, J = 1.8, 3H); ^{13}C NMR (D_2O, pD < 2): δ = 33.4, 53.5, 55.3, 122.1, 127.2, 145.5 ppm. LR-ESI(+)-MS calcd m/z for $C_{21}H_{32}GaN_9$ $(M-H)^{2+}$: 239.5, found: 239.5.

*^{nat}Ga NODIA-Me-NH-Me (Ga-**5**)*

NODIA-Me-NH-Me **5** (20 mg, 0.05 mmol) and gallium nitrate hydrate (66 mg, 0.26 mmol) were each dissolved in 500 µL sodium acetate buffer (0.1 M, pH 4.0), combined and heated at 95 °C for 30 min. After cooling to r.t., the ^{nat}Ga complex Ga-**5** was purified by semi-preparative RP-HPLC to give the final product as colorless powder after lyophilization (110 mg, 0.24 mmol, 95%). ^{1}H NMR (D_2O, pD < 2): δ = 2.96 (s, 3H), 3.03 (m, 2H), 3.15 (m, 2H), 3.27 (m, 2H), 3.57 (m, 6H), 3.71 (s, 6H), 4.18 (s, 2H), 4.58 (d, J = 17.1, 2H), 4.68 (d, J = 16.8, 2H), 6.75 (s, 2H), 7.39 (d, J = 1.7, 2H); ^{13}C NMR (D_2O, pD < 2): δ = 28.0, 33.3, 53.2, 53.5, 53.9, 55.5, 59.5, 122.2, 127.2, 145.8, 172.2 ppm. HR-ESI(+)-MS calcd m/z for $C_{19}H_{30}N_8O$ $(M-2H)^+$: 455.1798, found: 455.1796. RP-HPLC (semi-preparative, conditions B): t_R = 9 min.

*^{nat}Ga(Cl) NODIA-Me-NH-Me (Ga(Cl)-**5**)*

For preparation of the chloro complex, Ga-**5** (50 mg, 0.11 mmol) was incubated in 500 µL of a 1 M sodium chloride solution (pH 5.0) at 95 °C for 30 min. After lyophilization, Ga(Cl)-**5** was characterized by FT-IR and far-infrared IR (F-IR): ν = 257, 288, 386, 427, 417, 514, 574, 613, 660, 672, 704, 716, 795, 893, 919, 972, 1005, 1025, 1086, 1122, 1161, 1291, 1317, 1362, 1412, 1471, 1512, 1569, 1683, 1734, 2962 cm^{-1}.

*NODIA-Me-PSMA tert-butyl ester (Glu-CO-Lys(Ahx)-NODIA-Me-(tBu)$_3$ ester) (**6**)*

NODIA-Me **4** (10.0 mg, 0.027 mmol), HATU (12.2 mg, 0.032 mmol) and DIPEA (6.9 mg, 93 µL, 0.053 mmol) were dissolved in 200 µL DMF and the mixture was stirred for 30 min at room temperature. Then, Glu-CO-Lys(Ahx)-(tBu)$_3$ ester (16 mg, 0.027 mmol) in 100 µL DMF was added and the reaction mixture was stirred for additional 4 h. The solvent was removed as described for **5** and the residue was dissolved in 3 mL of water:acetonitrile 0.1% TFA (50:50) and purified by semi-preparative RP-HPLC (conditions A). Fractions containing the product were combined followed by rotary evaporation of acetonitrile under vacuum. The remaining aqueous phase was then lyophilized to give NODIA-Me-PSMA tert-butyl ester ((15*S*,19*S*)-tri-*tert*-butyl 1-(4,7-bis((1-methyl-1*H*-imidazol-2-yl)methyl)-1,4,7-triazonan-1-yl)-2,9,17-trioxo-3,10,16,18-tetraazahenicosane-15,19,21-tricarboxylate) **6** as colorless solid (9 mg, 0.01 mmol, 36%). RP-HPLC (semi-preparative, conditions A): t_R = 35 min. LR-ESI(+)-MS calcd m/z for $C_{48}H_{84}N_{11}O_9$ $(M+H)^+$: 959, found: 958.8.

*NODIA-Me-PSMA (Glu-CO-Lys(Ahx)-NODIA-Me) (**7**)*

NODIA-Me-PSMA tert-butyl ester **6** (9 mg, 0.01 mmol) was dissolved in 2 mL 5 M hydrochloric acid and the mixture allowed to stir for 16 h at room temperature. The reaction mixture was concentrated by rotary evaporation to a volume of 1 mL and further purified by semi-preparative RP-HPLC to give NODIA-Me-PSMA ((15*S*,19*S*)-1-(4,7-bis((1-methyl-1*H*-imidazol-2-yl)methyl)-1,4,7-triazonan-1-yl)-2,9,17-trioxo-3,10,16,18-tetraazahenicosane-15,19,21-tricarboxylic acid) **7** as colorless powder after lyophilization (7.2 mg, 9 µmol, 91%). HR-ESI(+)-MS calcd m/z for $C_{36}H_{60}N_{11}O_9$ $(M+H)^+$: 790.4576, found: 790.4564. RP-HPLC (semi-preparative, conditions B): t_R = 14:50 min; RP-HPLC (analytical, UV: 220 nm): t_R = 9:30 min.

*^{nat}Ga NODIA-Me-PSMA (Ga(Cl)-**7**)*

NODIA-Me-PSMA **7** (500 µg, 0.63 µmol) in 250 µL water and 950 µL ^{nat}Ga stock (1 mM $Ga(NO_3)_3$ in 5 mM HCl) were mixed in 1.5 mL in sodium acetate buffer (0.1 M, pH 4.0) and the mixture was heated at 95 °C for 30 min. After cooling to r.t., the ^{nat}Ga complex Ga(Cl)-**7** was purified using a C_{18} Sep-Pak cartridge (Waters), which was preconditioned using 5 mL of ethanol followed by 5 mL of water. After loading of the reaction mixture, the cartridge was washed with 2 mL of water and the product was eluted off using 2 mL ethanol:water (50:50 v/v). HR-ESI(+)-MS calcd m/z for $C_{36}H_{57}GaN_{11}O_9$ $(M-2H)^+$: 856.3597, found: 856.3583. RP-HPLC (analytical, UV: 220 nm): t_R = 9:39 min.

*^{nat}Ga NODIA-Me-PSMA (Ga(OH)-**7**)*

NODIA-Me-PSMA **7** (100 µg, 0.13 µmol) in 50 µL water and 20 µL ^{nat}Ga stock (10 mM $Ga(NO_3)_3$ in 5 mM HNO_3) were mixed in 200 µL in sodium acetate buffer (0.1 M, pH 4.5) and the mixture was heated at 95 °C for 15 min. After cooling to r.t., the ^{nat}Ga complex Ga(OH)-**7** was purified

similarly to Ga(Cl)-**7** using a C_{18} Sep-Pak cartridge (Waters). HR-ESI(+)-MS calcd m/z for $C_{36}H_{57}GaN_{11}O_9$ $(M+H)^+$: 856.3597, found: 856.3585. RP-HPLC (analytical, UV: 220 nm): t_R = 9:20 min.

Radiolabelling Experiments

For the preparation of ^{68}Ga complexes, stock solutions of the ligands NOTI-Me, NOTThia and NOTA were prepared in labelling buffer (sodium acetate 0.2 M pH 4.0). In a typical experiment, 2.5 - 10 µL of chelator stock solution (corresponding to a final concentration of 0.5 µM – 10 µM) were mixed in the appropriate amount of labelling buffer followed by the addition of 50 µL (~5 – 10 MBq $^{68}GaCl_3$) generator eluate to give a final volume of 500 µL. After brief mixing, samples were either incubated at room temperature or 95 °C for 15 minutes. Analysis was initially performed by analytical RP-HPLC. The radiochemical conversion (RCC) was also checked by TLC using silica gel microfiber strips (Agilent, iTLC-SG glass microfiber) and DTPA solution (50 mM, pH 7.4). Prior to the labelling experiments, additional tests were performed by TLC in which we used the ^{68}Ga eluate without the presence of our ligands to exclude the formation of any colloidal gallium hydroxide. No differences between the HPLC and TLC analyzed samples were observed so that determination was continued by TLC. While ^{68}Ga-NOTI-Me (^{68}Ga-**1)** and ^{68}Ga-NOTThia (^{68}Ga-**2)** remained at the origin (R_f = 0), uncomplexed ^{68}Ga (in the form of the corresponding DTPA complex) moved with the solvent front (R_f = 1). Strips were then analyzed by phosphorimaging and RCC was calculated. Each experiment was performed at least in triplicate.

*^{68}Ga NODIA-Me-PSMA (^{68}Ga-**7**)*

^{68}Ga radiolabelling of the bioconjugate **7** was conducted by using the Modular-Lab PharmTracer automated synthesis module (Eckert&Ziegler, Berlin, Germany). Briefly, the ^{68}Ge/^{68}Ga-generator (Eckert&Ziegler, Model IGG100 Gallium-68 Generator) was eluted with 0.1 M HCl (7 mL) in accordance with the manufacturer's protocol. The eluate (~600 MBq) was loaded onto a cation exchange column (Strata-XC [SCX], Phenomenex, Torrance, USA) and ^{68}Ga was eluted from the SCX cartridge with 800 µL of a mixture of 0.13 M HCl in ~5 M NaCl(aq.) into the reaction vial. The reaction vial contained 20 µg NODIA-Me-PSMA **7** in a mixture of 400 µL sodium acetate buffer (pH 4.5) and 2 mL water. Labelling was accomplished by heating the reaction mixture at 95 °C for 10 min. For purification, the solution was then loaded onto a C_{18} light cartridge (Waters, Milford, USA), which was washed with 3 mL saline and eluted with 1 mL 50 % ethanol. The final product was constituted by addition of 3 mL saline and sterilized by filtration using Millex 0.22 µm filter (Millipore, Billerica, USA). RP-HPLC (analytical, radioactivity detector): t_R = 9:40 min. The product ^{68}Ga-**7** was obtained in a decay corrected radiochemical yield (RCY) of ≥98% (n = 10) and a radiochemical purity (RCP) of ≥98% with a specific activity of A_s = 31.2±1.2 MBq nmol^{-1}.

Lipophilicity (log D) measurements

For log D measurements, 1–2 MBq of ^{68}Ga-**7** in saline (20 µL) was added to a mixture of phosphate buffered saline pH 7.4 (PBS) (480 µL) and octanol (500 µL) in 1.5 mL Eppendorf tubes. Samples were shaken for 1 h at room temperature. For separation, the samples were then centrifuged at 13200 rpm for 5 min. From each phase, 100 µL were transferred into plastic tubes, and the radioactivity of the samples was counted using a Wizard Gamma Counter (Perkin Elmer). Experiments were performed in triplicate.

DTPA challenge measurements

7–9 MBq (10 µL) of ^{68}Ga-**7** were added into 200 µL of 50 mM DTPA solution pH 7.4 (diethylenetriamine penta-acetic acid) and the mixture was stored at room temperature. At selected time points, 20 µL samples were drawn and analyzed by analytical RP-HPLC. The percentage of intact ^{68}Ga-**7** conjugates was calculated from the HPLC chromatograms. Experiments were performed in triplicate.

Serum stability and protein binding measurements

For each experiment, 7–9 MBq (10 µL) of ^{68}Ga-**7** were added to human serum (1 mL, human male AB plasma, Sigma-Aldrich) in a 1.5 mL Eppendorf tube, which was pre-equilibrated at 37 °C in a cell incubator for 1 h. Samples were vortexed and stored at 37 °C in a cell incubator. At selected time points, 100 µL aliquots were taken from the serum solution and serum proteins removed by centrifugation using centrifuge tubes (Vivacon 500; 30 kDa molecular weight cut-off; Sartorius Stedium Biotech, Göttingen, Germany) at 4 G for 5 min at 4 °C. To the filter, 100 µL PBS were added followed by an additional centrifugation step. For determination of protein bound fraction, the filters and the filtrates were transferred into plastic tubes, and samples were counted using a Wizard Gamma Counter. A sample of the filtrate was kept on ice until HPLC analysis. The percentage of intact ^{68}Ga-**7** conjugates was calculated from the HPLC chromatograms. All experiments were performed in triplicate.

Small animal PET Imaging

Small animal PET studies were carried out in accordance with the German Animal License Regulations and were approved by the animal care committee of the Regierungspräsidium Freiburg. Imaging was performed on a Focus 120 microPET scanner (Siemens Medical Solutions, USA). For PET imaging studies, nude mice (balb/c nude, Janvier Labs, Le Genest-Saint-Isle, France) (n = 3) were anesthetized with isoflurane (2-4% in air) and placed on the scanner. Immediately after scan start, animals were injected with 100 µL of ^{68}Ga-**7** (~3.7 MBq) in saline via a catheter into a the tail vein. Data were acquired for 60 min in list mode. Reconstruction was performed using unweighted OSEM2D. Image analysis was performed using AMIDE. Time-activity curves (TACs) were constructed by manually drawing regions of interest (ROI) over the heart, the liver, the kidneys and the bladder. All ROIs were then copied on each of the frames, and time-activity curves of the ROI mean values were generated.

Computational details

All calculations were conducted by using DFT as implemented in either the Gaussian03W Revision B.04 or Gaussian09 Revision B.01 suite of *ab initio* quantum chemistry programs.[49] Normal self-consistent field (SCF) and geometry convergence criteria were employed throughout. Structures were optimized in the gas phase without the use of symmetry constraints. Harmonic frequency analysis based on calculated analytical second derivatives was used to characterize optimized structures as local minima. All calculations employed the B3LYP[50-52] exchange-correlation functionals with either the LANL2DZ[53-56] or DGDZVP[57-59] basis sets.

Solvation effects were incorporated[60-61] iteratively *via* self-consistent reaction field (SCRF) calculations using the integral equation formalism polarisable continuum model (IEFPCM).[62] Due to limitations in computational capacity, full geometry optimizations in the presence of the solvent

field were beyond our capacity. Therefore, optimized gas phase geometries were used as input structures for single point calculations incorporating the solvent reaction field. The influence of full geometry relaxation in the continuum solvent model is expected to be minor.[63] The solute-solvent boundary was defined by using a solvent excluding surface (SES).[64] The molecular solute surface was defined by using the United Atom Topological model (UAHF) for the radii of the solute atoms.[65] Water was used as a solvation model (dielectric constant, ε = 78.3553) which reflects the experimental medium used in the radiosynthesis and application of ^{68}Ga-labelled PET radiotracers. Natural Bond Order (NBO) was performed using default parameters. Optimized structures and molecular orbitals were analyzed by using Chemcraft (version 1.7, build 382).

Results and Discussion

In combination with additional donor groups, the preorganized geometry of the TACN ring, with its small ring size, appears to be optimal for complexation of small metal cations like Ga^{3+}. On the other hand, the hard Lewis acid Ga^{3+} generally prefers hard, charge compensating oxygen donors such as carboxylates, phosphonates, phosphinates, etc.[28, 66] However, there are also a few examples of ligands in the literature with rather soft donor atoms such as thiolates that form stable Ga complexes including TACN-TM (= 1,4,7-tris(2-mercaptoethyl)-1,4,7-triazacyclononane) and 6SS (= *N*,*N'*-bis(2,2-dimethyl-2-mercaptoethyl)ethylenediamine-*N*,*N'*-diacetic acid).[67-69] We recently described the synthesis of a novel class of hexadentate ligands for tailored complexation of radioactive Cu^{2+} ions. These chelators are also based on the nine-membered TACN macrocycle and include up to three five-membered azaheterocycles such as imidazole and thiazole as additional donor groups.[45] In particular, imidazole is considered to be a moderate σ-donor and a weak π-acceptor, with electron donating properties that are intermediate between those of saturated amines such as ammonia and unsaturated amines such as pyridine.[70] Moreover, thiazole is considered to be more aromatic than imidazole.[71] In the spectrochemical series, both ligands are ranked above oxygen donors and below ammonia and pyridine and both ligands can be classified as borderline N donors.[70, 72] We therefore sought to investigate the complexation properties of this novel class of ligands with $^{nat/68}Ga^{3+}$ and evaluate its potential for future use in radiopharmaceutical applications.

Ligand and ^{nat}Ga Complex Syntheses

Initial screening was performed on the trisubstituted derivatives NOTI-Me **1** and NOTThia **2** (Scheme 2), which were prepared as previously described.[45] Both ligands, however, lack a

functionality that allows covalent linkage to a targeting vector. A well-established method for covalent conjugation of a BFC to a targeting vector is the formation of a peptide bond between a carboxylic acid function of the BFC and an amino group of the biomolecule. Hence, we synthesized the BFC NODIA-Me **4** (Scheme 2), where we replaced one of the pendent azaheterocyclic arms of the original chelating system with an acetic acid residue to provide the possibility for the conjugation of biomolecules, while maintaining the complexation properties of this class of chelators. For the preparation of **4**, the disubstituted compound **3** (NODI-Me) was used as starting material, which can be obtained during the synthesis of NOTI-Me **1**.[45] Reaction of **3** with glyoxylic acid in the presence of the reducing agent sodium triacetoxyborohydride gave the BFC NODIA-Me **4** in 90% yield (Scheme 3).[73] For more detailed studies on the complex formation with $^{nat}Ga^{3+}$, we also prepared the ligand NODIA-Me-NH-Me **5** (86%) as a model compound, in which the carboxylic acid was reacted with methylamine and HATU in order to mimic conjugation of a targeting vector by formation of an amide bond (Scheme 3). The corresponding Ga complex Ga-**5** was also employed in the DFT calculations (*vide infra*). All ligands were fully characterized by 1D- and 2D NMR spectroscopy and mass spectrometry and their purity (>98%) was confirmed by analytical RP-HPLC. In order to assess the potential of this novel BFC *in vivo*, we conjugated NODIA-Me **4** using HATU to the commercially available precursor Glu-CO-Lys(Ahx)-$(tBu)_3$ (Scheme 3). After deprotection of the intermediate **6** in 5 M HCl and purification by semi-preparative HPLC, the final PSMA-targeting bioconjugate **7** was obtained in 33% overall yield. The identity of compound **7** was confirmed by high resolution MS and its purity (>98%) was determined by analytical HPLC. For more detailed studies on the complex formation with Ga^{3+} and as reference compounds, complexes Ga-**1**, Ga-**5** and Ga-**7** were prepared by mixing equal

amounts of ligand and gallium nitrate stock solutions followed by heating at 95 °C for 30 min. All characterization data are given in the Supporting Information.

^{68}Ga Labelling Experiments

For radiopharmaceutical applications, sufficient binding of the radiometal of interest is essential. In this respect, we initially determined the Ga complexation properties of the imidazole **1** and thiazole **2** derivative in comparison to the ligand NOTA in ^{68}Ga labelling experiments (Figure 1). Labellings were performed manually at pH 4.0 in sodium acetate buffer to avoid the formation of insoluble gallium hydroxide. The investigated chelator concentration range of 0.5 µM – 10 µM corresponds to specific activities of A_s = ~2 – 40 MBq nmol^{-1}. The ligand NOTI-Me **1** bearing 2-methylimidazole substituents labelled readily with ^{68}Ga in sufficient specific activities, even at ambient temperatures. Increasing the temperature to 95 °C resulted in a higher RCC and accordingly in higher specific activities. In contrast, the thiazole derivative NOTThia **2** did not label with ^{68}Ga. Even at increased ligand concentrations and elevated temperatures no quantitative RRC could be achieved rendering thiazole type N donors unsuitable for Ga^{3+} complexation. The ligand NOTA, which is known to label under ambient temperatures[74], on the other hand, gave quantitative RCCs at room temperature with specific activities of ~20 MBq nmol^{-1}.

To demonstrate further the applicability of these novel chelators for envisaged radiopharmaceutical applications, we also performed ^{68}Ga labelling of the PSMA-targeting bioconjugate **7** incorporating the BFC NODIA-Me **4** in a fully automated, GMP compliant process using the Eckert&Ziegler Pharmtracer module in combination with sterile single-use cassettes. Prior to the labelling reaction, the generator eluate (~600 MBq) was concentrated and purified by trapping on a cation exchange cartridge in accordance with previously reported methods.[75]

Labelling of the bioconjugate **7** was performed in sodium acetate buffer (pH 4.5) at 95 °C for 10 min. After purification using a C_{18} Sep Pak cartridge, the product ^{68}Ga-**7** was obtained in a decay corrected radiochemical yield (RCY) of ≥98% (n = 10) and a radiochemical purity (RCP) of ≥98% with a specific activity of A_s = 31.2±1.2 MBq nmol^{-1}. Labelling of our novel chelators requires slightly higher ligand concentrations or heating to achieve specific activities comparable to those obtained using NOTA. Nonetheless, the determined conditions for quantitative labelling and corresponding specific activities are more than sufficient for future radiopharmaceutical applications and the results of the labelling experiments clearly demonstrate the capability of these novel chelators to complex ^{68}Ga, even under acidic conditions and ambient temperature.

Structures of ^{nat}Ga complexes in solution

In order to learn more about the metal binding properties of these novel chelates in solution, we performed a series of 1D- and 2D-NMR experiments on Ga-**1** as well as on the model compound Ga-**5**. As expected, the ^{1}H spectrum of the ligand NOTI-Me **1** at pD < 2 in Figure 2A shows only four resonances at 3.14 ppm (CH_2 groups of TACN), 3.87 ppm (CH_3 imidazole), 4.42 ppm (CH_2 bridging) and 7.47 ppm (imidazole protons). The corresponding ^{1}H spectrum of Ga-**1** in Figure 2B (pD < 2) significantly differs to that of the free ligand **1** consistent with the formation of a highly symmetric, hexadentate 1:1 chelate with a local C_3 symmetry in solution. Upon Ga^{3+} coordination, the decrease of macrocycle flexibility results in a splitting of the CH_2 resonances of the TACN macrocycle into a set of three multiplets in the range of ~2.7 – 3.7 ppm, which is consistent with an AA'MX coupling pattern, corresponding to a slow (δδδ) ⇔ (λλλ) ring conformational interconversion on the NMR time scale. In addition, the CH_2 groups of the methylimidazole arms exhibit an AB coupling pattern consistent with their non-equivalence due to the long lifetime of

the corresponding Ga-N bonds on the NMR time scale. Interestingly, the imidazole protons shifted to higher field, in which the proton adjacent to the metal coordinated N donor is strongly shielded, which can be attributed to the ring current caused by the anisotropic effect of the aromatic imidazole rings. This contrasts with the Ga(NOTA) complex, in which the diasterotopic CH_2 groups of TACN gave symmetrical multiplets at 3.23 and 3.51 ppm, corresponding to a well resolved AA'MM' multiplet pattern consistent with a fast conformational change of the TACN ring protons.[76] Furthermore, the protons of the CH_2 groups of the acetic acid residues gave a singlet at 3.88 ppm, consistent with a short Ga-O bond lifetime on the NMR time scale.[76] The splitting pattern of Ga-**1** is comparable to that of $Ga(NOTP)^{3-}$ (NOTP = 1,4,7-triazacyclononane-1,4,7-tri(methylenephosphonate)) with inert Ga-O bonds and quite strong Ga-N bonds.[77] In this respect, the presented NMR data for Ga-**1** confirms formation of a rigid 1:1 complex with strong Ga-N TACN bonds and inert Ga-N bonds to the imidazole residues.

While compound **1** is a hexadentate ligand able to saturate the octahedral coordination sphere around the Ga^{3+} cation, the BFC NODIA-Me **4** provides only five donor atoms if the remaining acetic acid function is used for conjugation of biologically active molecules and, thus, leaving one coordination site of an octrahedral coordination unoccupied. During the HPLC characterization of ^{68}Ga-**7**, we observed the formation of another species in chloride free medium and at basic pH, which we attributed to an exchange of weakly coordinating, monodentate ligands such as chloride and hydroxide anions (*vide infra*). We therefore sought to investigate the coordination geometry of Ga-**5** in more detail by NMR spectroscopic studies (Figure 2C and 2D). The proton NMR of the free ligand **5** in Figure 2C shows three broad multiplets for the TACN protons at 2.77, 3.07 and 3.42 ppm. The singlet resonance at 2.86 ppm corresponds to the terminal CH_3 group of the amide bond and the singlet at 3.91 ppm to the two CH_3 groups of the imidazole residues. The CH_2 signals

at 4.18 ppm and 4.23 ppm correspond to the CH_2 groups of the acetate and methylimidazole arms, respectively. The protons of the imidazole resonate as doublets at 7.55 and 7.56 ppm. When coordinated to Ga^{3+} (pD < 2), the TACN resonances split into four multiplets for the equatorial and axial protons as seen in Figure 2D. This is representative for an ABMX coupling pattern, confirming a slow TACN ring conformational interconversion for Ga-**5**. Similar to Ga-**1**, the protons of the CH_2 groups of the methylimidazole arms show an AB coupling pattern, consistent with an inert binding of the imidazole N donors to the metal center. The imidazole proton adjacent to the coordinated N donor is also strongly shielded as already seen for Ga-**1**. Interestingly, the CH_2 protons of the carboxy function show a singlet at 4.18 ppm, which is not significantly shifted in comparison to the signal of the free ligand (4.18 vs. 4.23 ppm both in MeOD, see Supporting Information). This is consistent with no involvement of the amide function in metal binding because one would expect to see a shift of the corresponding resonance upon coordination to the metal center, even considering a short lifetime of the corresponding amide-N or carbonyl-O interaction. However, the presence of a singlet might also be attributed to the C_s symmetry of the Ga-**5** complex. Nonetheless, from these results a fast exchanging coordination via the carbonyl-O or amide-NH in solution cannot entirely be excluded. In the proton NMR of Ga-**5** in MeOD (Supporting Information), additional resonances for both imidazole protons and the methyl groups were obtained, while all other signals were not doubled. Obviously, two separate species are present in MeOD in the ratio of 5:1. The fact that only resonances of the methylimidazole residues are doubled indicates differences in close proximity to these protons. Since complex Ga-**5** was prepared in the absence of chloride under acidic conditions, coordination of a water molecule or of the amide group might explain the presence of additional resonances. Altogether, the proton NMR of Ga-**5** shows the formation of a 1:1 chelate with a slow conformational interconversion of

the macrocycle and inert Ga-N bonds for the imidazole donors. Even though the exact determination of the occupancy of the remaining coordination site was not possible by these experiments, it can be concluded that both ligands **1** and **5**, in contrast to NOTA, form highly rigid complexes with Ga^{3+}. It is also noteworthy that protonation of imidazole residues or even decomplexation at acidic pH (pD < 2) was not seen in the characterization of either Ga-**1** or Ga-**5**.

Stability Measurements

Kinetic stability of the corresponding metal complex under biologically relevant conditions is essential for radiopharmaceuticals in order to avoid premature loss of the radiometal and/or transchelation *in vivo*. In addition to the NMR studies that revealed formation of rigid 1:1 chelates for ligands **1** and **5**, we furthermore determined the stability of the conjugate ^{68}Ga-**7** *in vitro* by ligand challenge (DTPA) and serum stability studies (Figure 3). In saline and PBS, the product of the radiolabelling of **7** (assigned to ^{68}Ga(Cl)-**7**; *vide infra*) was found to be stable for >4 h with respect to changes in RCP as determined by HPLC. These observations confirmed that no radiolysis or chemical degradation occurred during the course of the experiment (Figure 3A). Stability was further assessed by incubation in DTPA solution (50 mM, pH 7.4) at room temperature. No transchelation was noted for >4 h (Figure 3B), indicating that the ^{68}Ga complex remained stable (~3% transchelation after 4 h, t_R (^{68}Ga-DTPA) = 2:4 min). However, at a pH > 7 and in the absence of chloride anions, e.g. incubation in DTPA solution at pH 7.4 as for the ligand challenge experiment, formation of another species (t_R = 9:20 min) (assigned to ^{68}Ga(OH)-**7**; *vide infra*) that eluted just prior to the product peak (t_R = 9:40 min) was noted. Over time, this newly formed species increased from ~1% at 15 min after synthesis to ~17% at 4 h (Figure 3B). A similar finding was observed in the serum stability study (pH > 7). After incubation in human serum at 37

°C for 1 h, the species giving rise to the new peak (t_R = 9:20 min) was formed to ~20% and increased up to ~65% after 4 h (Figure 3C+D). Interestingly, apart from the formation of this new species, no significant degradation was observed (~1%) for up to 4 h. The protein associated fraction of ^{68}Ga-labelled **7** was low at 14.6 ± 1.0% (n = 3). Overall, no activity associated with either a fully hydrolyzed $[^{68}Ga(OH)_4]^-$ or $[^{68}Ga(DTPA)]^{2-}$ (both of which elute at the solvent front in the HPLC analysis) was observed in the stability measurements indicating that the gallium ion remained bound to the macrocyclic chelate under these conditions. Further, the close retention times between the initial ^{68}Ga(Cl)**-7** product and the new species suggested that the two species were extremely similar in size, shape and polarity.

Studies on the Interconversion of ^{68}Ga-7

In general, Ga^{3+} cations in aqueous medium exhibit a preference for hexadentate coordination typically in an octahedral fashion.[28] The ligand NODIA-Me **4** only provides five donor atoms for metal chelation and is consequently not capable of saturating the coordination sphere around the Ga^{3+} cation. As indicated, the fact that the retention time difference between the parent ^{68}Ga(Cl)-**7** (9.40 min) and daughter (9.20 min) peaks was so close suggested that only a minor change in structure or polarity was occurring. Our hypothesis was that the remaining coordination site might be occupied by various monodentate ligands such as chloride, water, hydroxide ions, etc. or by the carbonyl oxygen atom of the adjacent peptide bond and that an interchange between two of such species occurs. Since the radiolabelling of **7** was performed in the presence of an excess of chloride ions (from the eluent used to wash off the $^{68}Ga^{3+}$ activity after trapping on the strong cation exchange (SCX) cartridge), our assumption was that the remaining coordination site of ^{68}Ga-labelled **7** is occupied by a chloride ion at the end of radiolabelling after final purification and

formulation in saline. Furthermore, we found that under neutral or slightly acidic conditions (pH ≤ 7.0), e.g. as in the product formulation or PBS, no conversion of ^{68}Ga-**7** to the daughter species at 9.20 min occurred over a period of 4 h.

To probe the involvement of chloride ions as potential ligands, we performed further experiments. First, ^{68}Ga-**7** corresponding to the parent peak at 9.40 min was reacted with a solution of $AgNO_3$(aq.). Sequestration of the chloride in solution led to quantitative conversion of the parent species (9.40 min) into the daughter product at 9.20 min (Figure S29). This reaction provided a strong indication that the formulated ^{68}Ga complex contains a chloride anion, likely acting as a ligand and/or alternatively bound closely to the metal complex as a counter ion. Second, we prepared the corresponding non-radioactive Ga conjugates with and without chloride anions present in the reaction mixture and analyzed the products by RP-HPLC. The retention time in the UV chromatogram of the Ga complex with chloride anions present matched that observed for the radioactive ^{68}Ga-labelled **7** species obtained at the end of the radiosynthesis. In contrast, the Ga complex prepared without chloride anions in the reaction conditions eluted with a shorter retention time (9.20 min) consistent with the formation of the new daughter species seen in the studies using radioactive gallium (Figures S30 and S31). All attempts to identify the coordination of either a chloride or a hydroxide ion bound to the ^{nat}Ga-**5** complex using HRMS (high resolution mass spectrometry) were unsuccessful. Absence of a peak in HRMS is not confirmative and is potentially due to the labile coordinating character of both ions that may result in decomposition even under mild electrospray ionization conditions. Also, attempts to obtain single crystals of the model compound Ga-**5** were not successful. Nonetheless, as indicated by DFT calculations (*vide infra*), if the two species (parent and daughter) are in equilibrium it should be possible to regenerate the parent peak (9.40 min) at pH < 7 in the presence of an excess chloride anions. Incubation of an

aliquot of a solution containing both the parent and daughter peak at pH 5.0 in the presence of excess sodium chloride resulted in formation of a single 'parent' peak. Representative HPLC chromatograms are given in Figure S32. The substitution reaction was also found to be pH dependent. Regeneration to the parent peak at 9.40 min could only be achieved below pH ≤ 7, which provides additional support that the daughter peak involves the formation of a ^{68}Ga-hydroxide complex. Furthermore, coordination of a chloride anion to Ga-**5** could be confirmed by far infrared (F-IR) measurements. The corresponding F-IR spectrum of Ga-**5** in the presence of chloride (Figure S33) shows an absorbance at ~387 cm^{-1}, which is assigned to a Ga-Cl stretching vibration.[47, 78] In a structurally similar Ga complex, the IR spectrum showed a Ga-Cl stretching vibration at 375 cm^{-1}.[79] This is also in accordance with the calculated IR spectra from our DFT calculations on different coordination modes of Ga-**5** (Figure S35). The Ga-N stretching vibrations of the imidazoles at 210 and 258 cm^{-1} are in close agreement to vibrations of 227 and 248 cm^{-1} for a previously reported Ga imidazole complex.[47] According to the IR measurements, the carbonyl group of the amide function does not bind to the metal in the solid state. The measured IR band of 1683 cm^{-1} is comparable to the C=O stretching frequencies reported for acetamide and *N*,*N*-dimethylformamide.[80-82]

To investigate the potential ligand substitution reaction in more detail, we additionally performed a series of kinetic studies using different concentrations of initial ^{68}Ga complex, varying pH, and different temperatures. Since the use of NaCl in the radiolabelling reaction was unavoidable, and attempts to remove chloride from the formulation using e.g. Ag Sep-Pak cartridges led to the exclusive formation of the daughter peak, it was not possible to control the chloride ion concentration in a systematic way. The presence of a relatively high concentration of

NaCl in the formulation meant that reactions were essentially conducted under pseudo-first order conditions with respect to chloride ion concentration.

Increasing the concentration of the ^{68}Ga complex by a factor of 10 was found to increase the rate of daughter peak formation from an initial rate of 64 ± 2 pmol min^{-1} to 643 ± 27 pmol min^{-1} (Figure 4A). This 10-fold increase in absolute conversion rate indicates that the reaction is first-order with respect to the initial concentration of the parent ^{68}Ga(Cl)-**7**complex. This conclusion was also supported by a plot of relative percentage of the daughter over parent peak (%) vs. time which showed that the *relative* rate of transformation of the peak at 9.40 min into the daughter peak at 9.20 min was identical irrespective of the initial ^{68}Ga complex concentration (Figure 4B). In addition to confirming that the reaction is first order in ^{68}Ga concentration, this experiment demonstrated that the same reaction process occurs in the concentration window studied (i.e. no other species were identified in the radio-HPLC chromatograms), and also that the reaction does not lead to the formation of an intermediate (observable) dimeric Ga complex in the rate determining step, i.e. the daughter peak is likely monomeric in ^{68}Ga.

Next, the relative rate of reaction for conversion of the parent ^{68}Ga complex into the daughter species was measured at different pH values in 0.1 M HEPES buffer (Figure 4C). The first observation was that in the control medium (water at pH 5.5) no reaction occurred. This was also consistent with the experimental observation that the parent ^{68}Ga complex remains intact in the formulated product (saline; pH 5.5). However, at a pH > 7 and in the absence of chloride anions, the initial rate of conversion of parent into daughter species was found to increase when the pH of the buffer solution was increased in the range of 7.4 to 9.1. This observation supports the conclusions from the DFT calculations (*vide infra*) which predicted that the formation of a (*Z*)-Ga(OH)-**5** complex either *via* hydrolysis and reaction with (*Z*)-Ga-**5** or by ligand substitution from

(*Z*)-Ga(Cl)-**5** should be pH-dependent. Extrapolation of the data to estimate initial rates of reaction allowed the measurement of different values for log k_{obs}, and a subsequent plot of these observed rates constants *versus* log[OH^-] allowed the determination of the order of reaction with respect to hydroxide ion concentration (Figure 4D). Interestingly, the reaction was found to be non-linear in hydroxide concentration with a rate order, $n = 0.62 \pm 0.04$. In non-ideal systems, non-integer rate orders in H^+ or OH^- ions are common and typically indicate that either the reaction mechanism is complex or that multiple, competing pathways may be plausible.

Overall, the experimental data provide strong support that the exchange reaction can be assigned to a chloride-to-hydroxide ligand substitution. The reaction is pH dependent, first order in gallium and non-linear in hydroxide concentration. Detailed kinetic studies are required to fully assign the mechanism. These experiments are ongoing but this work is beyond the scope of the current report. Collectively, the experimental data provide plausible, if not yet conclusive support for assignment of ^{68}Ga(Cl)-**7** as the parent species and ^{68}Ga(OH)-**7** as the daughter species.

Computational Studies on the Complex Formation

In addition to the experimental data, we also performed Density functional theory (DFT) calculations to probe the nature of the Ga-**5** complex and the energetics of ligand substitution in more detail. Initial calculations investigated the energetic difference between the formation of a hexadentate complex with either *E* or *Z* isomerisation about the coordinated amide bond (Figure S36). DFT calculations predicted only a minor difference in free energy between the *E* and *Z* isomers. The *Z* isomer was calculated to be slightly more stable than the *E* isomer in both gas and solution phases independent of the used basis set. Subsequent calculations focused on the *Z* isomer.

It is plausible that the amide donor ligand in Ga-**5** could be labile giving either a penta-coordinate Ga complex or a hexacoordinated complex in which the amide donor is replaced by a solvent molecule (H_2O). Thus, we also investigated the possibility of solvent-induced structural isomerism (Figure S37). Unsurprisingly, dissociation of the Ga-amide coordination bond is energetically unfavorable with a calculated change in free energy of +109.4 kJ mol^{-1} (DGDZVP / water solvent model). Replacing the amide donor with a solvent molecule (H_2O) partially compensated for this energetic difference but the reaction remained non-spontaneous with a change in free energy calculated between +17.7 to +93.4 kJ mol^{-1} (depending on the nature of the $(H_2O)_n$ water cluster models used as energetic references). DFT calculations indicated that under pH neutral or acidic conditions, and in the absence of alternative donor ligands, the hexadentate (*Z*)-Ga-**5** complex involving the coordination of an amide oxygen donor ligand is likely the predominant species in solution.

The reaction conditions employed to synthesize and purify the ^{68}Ga-labelled NODIA-Me-PSMA complexes ^{68}Ga(Cl)-**7** include an acidic (HCl), saturated sodium chloride solution, with preparation and final formulation of the product in saline (*vide infra*). It is plausible that the formulated ^{68}Ga-complexes include chloride anions as counter ions and potentially as a coordinated donor ligand. Thus, DFT calculations were used to predict the possibility of forming an alternative, hexadentate (*Z*)-Ga(Cl)-**5** complex in which the amide donor is replaced by a chloride ligand (Figure S38). The calculated free energy change, ΔG(sol) / kJ mol^{-1}, in a water continuum solvent model for chloride ion addition to the (*Z*)-Ga-**5** varied between -41.1 to +5.8 kJ mol^{-1} depending on the nature of the water cluster model. For the majority of the water cluster models, DFT calculations indicate that substitution of the amide donor ligand with a chloride ligand is thermodynamically spontaneous (ΔG(sol) < 0 kJ mol^{-1}). This conclusion is consistent

with the electrostatic interaction between a 3+ charged Ga complex and a monoanionic chloride but also indicates that the Ga-Cl bond may be quite weak and labile.

Given the observed exclusive transformation of the parent species into a single daughter species under different conditions ($AgNO_3$, DTPA at pH > 7.4 and serum), we hypothesized that a pH-dependent hydrolysis may occur affecting a ligand substitution reaction from the (*Z*)-Ga(Cl)-**5** to give a (*Z*)-Ga(OH)-**5** complex. Calculated changes in free energy for the formation of the hydroxide complex from the (*Z*)-Ga-**5** complex *via* ligand exchange on the (*Z*)-Ga(Cl)-**5** complex are presented in Figure S39. In the case of chloride to hydroxide ligand exchange (Figure S40), two separate water cluster models were used for calculating the reference energies. Specifically, one water cluster $(H_2O)_n$, where n = 0 to 5, was used to calculate various solvated structures for the chloride ion upon release from the Ga complex. The second water cluster (n = 5) was required to provide a source of OH^- anion with the by-product being the solvated Eigen ion $H_9O_4^+$ which represents a commonly used approximation for a solvated proton. Again, the calculated change in free energy for Cl^- to OH^- ligand substitution was found to be dependent on the size of the water clusters used as an energy reference. Calculated ΔG(sol) values for the ligand substitution reaction varied from -9.7 to +37.1 kJ mol^{-1}. This relatively small change in free energy suggests that, *i*) the species are likely to be in equilibrium, and *ii*) the reaction is likely pH dependent. Overall, the DFT calculations are consistent with the assignment of (Z)-^{68}Ga(Cl)-**7** as the parent species (peak at 9.40 min) and (Z)-^{68}Ga(OH)-**7** as a daughter species (peak at 9.20 min).

Biodistribution Studies by Small-animal PET imaging

Finally, the stability of the radiolabelled bioconjugate ^{68}Ga-**7** was evaluated by small animal PET imaging in nude mice. Coronal MPIs (maximum intensity projections) of ^{68}Ga-**7** and

corresponding TACs (time activity curves) for organs of interest are given in Figures 5A and 5B, respectively. The bioconjugate ^{68}Ga-**7** exhibited fast blood clearance with an initial activity of ~40% IA g^{-1} (injected activity per gram) at 1 min p.i. (post injection) decreasing to ~13% IA g^{-1} at 10 min p.i. and essentially reaching background levels (~1.5% IA g^{-1}) after 1 h. Transferrin is an endogenous serum protein with two Fe^{3+} binding sites acting as iron transporter. Transferrin binds Fe^{3+} with high affinity but also displays high affinity for Ga^{3+}, which has a similar ionic radius to Fe^{3+}. Due to the rapid blood clearance of the bioconjugate ^{68}Ga-**7**, significant transchelation to transferrin does not occur confirming sufficient stability of the chelate *in vivo*. A similar uptake pattern was observed for the liver with ~25% IA g^{-1} at 1 min p.i. decreasing to ~9% IA g^{-1} at 10 min p.i. and ~1.6% IA g^{-1} after 1 h, respectively. The formulated radiolabelled bioconjugate **7** (assigned to ^{68}Ga(Cl)-**7**) was found to be highly hydrophilic with a log D value of -5.04 ± 0.36. The high hydrophilicity of ^{68}Ga-**7** is reflected in its rapid renal excretion via the kidneys. At 1 min p.i., ~26% IA g^{-1} were already present in the kidneys peaking at 15 min p.i. with ~120% IA g^{-1} followed by rapid excretion with ~4% IA g^{-1} at 1 h p.i.. In turn, the uptake in the bladder increased as the uptake in the kidneys decreases underlining the fast washout of ^{68}Ga-**7** from normal organs. Altogether, the biodistribution profile of ^{68}Ga-**7** matched that of an unretained but intact bioconjugate demonstrating high kinetic stability *in vivo*.

Conclusions

From the trisubstituted ligands NOTI-Me **1** and NOTThia **2**, only the imidazole derivative **1** labels with ^{68}Ga, while the thiazole derivative **2** does not bind the radiometal under identical conditions rendering thiazole N donors unsuitable for Ga complexation. Achieved specific activities are comparable to those of existing chelators such as NOTA. Replacement of one imidazole arm by an acetic acid residue provided the bifunctional derivative NODIA-Me **4** with a functionality that allows covalent conjugation of a targeting vector. The hexadentate chelator **1** as well as the pentadentate model compound **5** revealed the formation of rigid 1:1 chelates with Ga^{3+} at acidic pH in solution with a slow macrocyclic interconversion and inert Ga-N bonds for the imidazoles confirming strong metal binding. The BFC **4** was furthermore coupled to a PSMA targeting moiety to give the bioconjugate **7**. This was successfully labelled with ^{68}Ga in a fully automated, GMP compliant process in high RCY and RCP with a specific activity of ~30 MBq nmol^{-1}. Substitution of one imidazole arm by an acetic acid residue did not significantly alter the metal complex stability as demonstrated by serum stability and DPTA challenge experiments of the final ^{68}Ga labelled PSMA targeting bioconjugate **7**. More detailed investigations on these five-coordinate complexes revealed that the remaining/vacant coordination site of the octahedral Ga can be occupied by monodentate ligands such as chloride and hydroxide anions. Coordination of both monodentate ligands is concentration-dependent and these weakly associated ligands can undergo an exchange. Above pH 7 in the absence of chloride, coordination of hydroxide appears to be favored, whereas coordination of chloride occurs below pH 7 in the presence of chloride. This equilibrium is further supported by DFT calculations that revealed only small energetic differences for both complexes. In small animal PET imaging studies in healthy nude mice, the ^{68}Ga labelled PSMA targeting conjugate NODIA-Me-PSMA ^{68}Ga-**7** is rapidly excreted from normal organs

consistent with sufficient stability *in vivo*. Despite the fact that gallium remains strongly complexed by the ligand NODIA-Me, the formation/interconversion of two different complexes *in vitro* might be considered to be a disadvantage due to their potentially different biological properties such as binding affinity and biodistribution. On the other hand, dramatic differences in biological behavior are not expected due to the close similarity of both complexes in size, charge and lipophilicity. Moreover, the five-coordinate ligand NODIA-Me might also be a promising candidate for the radiofluorination of a preformed Ga complex.[79] More detailed *in vivo* studies of these chelators in combination with appropriate targeting vectors in tumor xenograft bearing mice will be reported. Investigations on the complex stability such as determination of formation constants are part of ongoing work. Notably, to the best of our knowledge, this is the first report of rigid and stable Ga imidazole complexes in aqueous media. Summarizing, TACN-based ligands bearing additional methylimidazole residues form stable complexes with ^{68}Ga and corresponding bifunctional derivatives show promise as chelating agents for the future development of gallium based radiopharmaceuticals.

Acknowledgements

JPH thanks the Department of Nuclear Medicine, University Hospital Freiburg, the German Cancer Consortium (DKTK), and the German Cancer Research Center (DKFZ) for financial support as well as the Swiss National Science Foundation (SNSF Professorship PP00P2_163683) and the European Research Council (ERC-StG-2015, NanoSCAN – 676904). MDB thanks the Chemistry Department of the Albert-Ludwigs-University Freiburg (Germany) for its technical support, in particular Luise Mintrop and Adrianna Kolberg for IR measurements, Christoph Warth for MS measurements. MDB thanks Prof. Philipp Kurz of the Chemistry Department of the Albert-Ludwigs-University Freiburg (Germany) for his continuous support. MDB also thanks the Research Commission of the University Freiburg as well as the Fonds der chemischen Industrie for funding.

References

1. Velikyan, I., 68Ga-Based radiopharmaceuticals: production and application relationship. *Molecules* **2015,** *20*, 12913-12943.
2. Velikyan, I., Prospective of (6)(8)Ga-radiopharmaceutical development. *Theranostics* **2013,** *4*, 47-80.
3. Banerjee, S. R.; Pomper, M. G., Clinical applications of Gallium-68. *Appl. Radiat. Isot.* **2013,** *76*, 2-13.
4. Morgat, C.; Hindie, E.; Mishra, A. K.; Allard, M.; Fernandez, P., Gallium-68: chemistry and radiolabeled peptides exploring different oncogenic pathways. *Cancer Biother. Radiopharm.* **2013,** *28*, 85-97.
5. Kumar, V.; Boddeti, D. K., (68)Ga-radiopharmaceuticals for PET imaging of infection and inflammation. *Recent Results Cancer Res.* **2013,** *194*, 189-219.
6. Varshney, R.; Hazari, P. P.; Fernandez, P.; Schulz, J.; Allard, M.; Mishra, A. K., (68)Ga-labeled bombesin analogs for receptor-mediated imaging. *Recent Results Cancer Res.* **2013,** *194*, 221-256.
7. Velikyan, I., The diversity of (68)Ga-based imaging agents. *Recent Results Cancer Res.* **2013,** *194*, 101-131.
8. Prata, M. I., Gallium-68: a new trend in PET radiopharmacy. *Curr Radiopharm* **2012,** *5*, 142-149.
9. Breeman, W. A.; de Blois, E.; Sze Chan, H.; Konijnenberg, M.; Kwekkeboom, D. J.; Krenning, E. P., (68)Ga-labeled DOTA-peptides and (68)Ga-labeled radiopharmaceuticals for positron emission tomography: current status of research, clinical applications, and future perspectives. *Semin. Nucl. Med.* **2011,** *41*, 314-321.
10. Decristoforo, C.; Pickett, R. D.; Verbruggen, A., Feasibility and availability of (6)(8)Ga-labelled peptides. *Eur. J. Nucl. Med. Mol. Imaging* **2012,** *39 Suppl 1*, S31-40.
11. Maecke, H. R.; Hofmann, M.; Haberkorn, U., 68Ga-Labeled Peptides in Tumor Imaging. *J. Nucl. Med.* **2005,** *46*, 172S-178S.
12. Rosch, F., (68)Ge/ (68)Ga generators: past, present, and future. *Recent Results Cancer Res.* **2013,** *194*, 3-16.
13. Taieb, D.; Garrigue, P.; Bardies, M.; Abdullah, A. E.; Pacak, K., Application and Dosimetric Requirements for Gallium-68-labeled Somatostatin Analogues in Targeted Radionuclide Therapy for Gastroenteropancreatic Neuroendocrine Tumors. *PET Clin* **2015,** *10*, 477-486.
14. Ambrosini, V.; Nanni, C.; Fanti, S., The use of gallium-68 labeled somatostatin receptors in PET/CT imaging. *PET Clin* **2014,** *9*, 323-329.
15. Kulkarni, H. R.; Baum, R. P., Theranostics with Ga-68 somatostatin receptor PET/CT: monitoring response to peptide receptor radionuclide therapy. *PET Clin* **2014,** *9*, 91-97.
16. Kulkarni, H. R.; Baum, R. P., Patient selection for personalized peptide receptor radionuclide therapy using Ga-68 somatostatin receptor PET/CT. *PET Clin* **2014,** *9*, 83-90.
17. Eder, M.; Schäfer, M.; Bauder-Wüst, U.; Hull, W.-E.; Wängler, C.; Mier, W.; Haberkorn, U.; Eisenhut, M., 68Ga-Complex Lipophilicity and the Targeting Property of a Urea-Based PSMA Inhibitor for PET Imaging. *Bioconjugate Chem.* **2012,** *23*, 688-697.
18. Afshar-Oromieh, A.; Malcher, A.; Eder, M.; Eisenhut, M.; Linhart, H. G.; Hadaschik, B. A.; Holland-Letz, T.; Giesel, F. L.; Kratochwil, C.; Haufe, S.; Haberkorn, U.; Zechmann, C. M., PET imaging with a [68Ga]gallium-labelled PSMA ligand for the diagnosis of prostate cancer:

biodistribution in humans and first evaluation of tumour lesions. *Eur. J. Nucl. Med. Mol. Imaging* **2013,** *40*, 486-495.
19. Eder, M.; Neels, O.; Muller, M.; Bauder-Wust, U.; Remde, Y.; Schafer, M.; Hennrich, U.; Eisenhut, M.; Afshar-Oromieh, A.; Haberkorn, U.; Kopka, K., Novel Preclinical and Radiopharmaceutical Aspects of [68Ga]Ga-PSMA-HBED-CC: A New PET Tracer for Imaging of Prostate Cancer. *Pharmaceuticals (Basel)* **2014,** *7*, 779-796.
20. Afshar-Oromieh, A.; Avtzi, E.; Giesel, F. L.; Holland-Letz, T.; Linhart, H. G.; Eder, M.; Eisenhut, M.; Boxler, S.; Hadaschik, B. A.; Kratochwil, C.; Weichert, W.; Kopka, K.; Debus, J.; Haberkorn, U., The diagnostic value of PET/CT imaging with the (68)Ga-labelled PSMA ligand HBED-CC in the diagnosis of recurrent prostate cancer. *Eur. J. Nucl. Med. Mol. Imaging* **2015,** *42*, 197-209.
21. Fendler, W. P.; Schmidt, D. F.; Wenter, V.; Thierfelder, K. M.; Zach, C.; Stief, C.; Bartenstein, P.; Kirchner, T.; Gildehaus, F. J.; Gratzke, C.; Faber, C., 68Ga-PSMA-HBED-CC PET/CT detects location and extent of primary prostate cancer. *J. Nucl. Med.* **2016,** *57*, 1720-1725.
22. Rauscher, I.; Maurer, T.; Beer, A. J.; Graner, F. P.; Haller, B.; Weirich, G.; Doherty, A.; Gschwend, J. E.; Schwaiger, M.; Eiber, M., Value of 68Ga-PSMA HBED-CC PET for the assessment of lymph node metastases in prostate cancer patients with biochemical recurrence: comparison with histopathology after salvage lymphadenectomy. *J. Nucl. Med.* **2016,** *57*, 1713-1719.
23. Prasad, V.; Steffen, I. G.; Diederichs, G.; Makowski, M. R.; Wust, P.; Brenner, W., Biodistribution of [(68)Ga]PSMA-HBED-CC in Patients with Prostate Cancer: Characterization of Uptake in Normal Organs and Tumour Lesions. *Mol. Imaging Biol.* **2016,** *18*, 428-436.
24. Pfob, C. H.; Ziegler, S.; Graner, F. P.; Kohner, M.; Schachoff, S.; Blechert, B.; Wester, H. J.; Scheidhauer, K.; Schwaiger, M.; Maurer, T.; Eiber, M., Biodistribution and radiation dosimetry of 68Ga-PSMA HBED CC-a PSMA specific probe for PET imaging of prostate cancer. *Eur. J. Nucl. Med. Mol. Imaging* **2016,** *43*, 1962-1970.
25. Weineisen, M.; Schottelius, M.; Simecek, J.; Baum, R. P.; Yildiz, A.; Beykan, S.; Kulkarni, H. R.; Lassmann, M.; Klette, I.; Eiber, M.; Schwaiger, M.; Wester, H.-J., 68Ga- and 177Lu-Labeled PSMA I&T: Optimization of a PSMA-Targeted Theranostic Concept and First Proof-of-Concept Human Studies. *J. Nucl. Med.* **2015,** *56*, 1169-1176.
26. Herrmann, K.; Bluemel, C.; Weineisen, M.; Schottelius, M.; Wester, H.-J.; Czernin, J.; Eberlein, U.; Beykan, S.; Lapa, C.; Riedmiller, H.; Krebs, M.; Kropf, S.; Schirbel, A.; Buck, A. K.; Lassmann, M., Biodistribution and Radiation Dosimetry for a Probe Targeting Prostate-Specific Membrane Antigen for Imaging and Therapy. *J. Nucl. Med.* **2015,** *56*, 855-861.
27. Chatalic, K. L.; Heskamp, S.; Konijnenberg, M.; Molkenboer-Kuenen, J. D.; Franssen, G. M.; Clahsen-van Groningen, M. C.; Schottelius, M.; Wester, H. J.; van Weerden, W. M.; Boerman, O. C.; de Jong, M., Towards Personalized Treatment of Prostate Cancer: PSMA I&T, a Promising Prostate-Specific Membrane Antigen-Targeted Theranostic Agent. *Theranostics* **2016,** *6*, 849-861.
28. Bartholomä, M. D., Recent developments in the design of bifunctional chelators for metal-based radiopharmaceuticals used in Positron Emission Tomography. *Inorg. Chim. Acta* **2012,** *389*, 36-51.
29. Velikyan, I.; Beyer, G. J.; Långström, B., Microwave-Supported Preparation of 68Ga Bioconjugates with High Specific Radioactivity. *Bioconjugate Chem.* **2004,** *15*, 554-560.

30. Blom, E.; Långström, B.; Velikyan, I., 68Ga-Labeling of Biotin Analogues and their Characterization. *Bioconjugate Chem.* **2009,** *20*, 1146-1151.
31. Decristoforo, C.; Hernandez Gonzalez, I.; Carlsen, J.; Rupprich, M.; Huisman, M.; Virgolini, I.; Wester, H.-J.; Haubner, R., 68Ga- and 111In-labelled DOTA-RGD peptides for imaging of αvβ3 integrin expression. *Eur. J. Nucl. Med. Mol. Imaging* **2008,** *35*, 1507-1515.
32. Griffiths, G. L.; Chang, C.-H.; McBride, W. J.; Rossi, E. A.; Sheerin, A.; Tejada, G. R.; Karacay, H.; Sharkey, R. M.; Horak, I. D.; Hansen, H. J.; Goldenberg, D. M., Reagents and Methods for PET Using Bispecific Antibody Pretargeting and 68Ga-Radiolabeled Bivalent Hapten-Peptide-Chelate Conjugates. *J. Nucl. Med.* **2004,** *45*, 30-39.
33. Ren, G.; Zhang, R.; Liu, Z.; Webster, J. M.; Miao, Z.; Gambhir, S. S.; Syud, F. A.; Cheng, Z., A 2-Helix Small Protein Labeled with 68Ga for PET Imaging of HER2 Expression. *J. Nucl. Med.* **2009,** *50*, 1492-1499.
34. Liu, Z.; Yan, Y.; Liu, S.; Wang, F.; Chen, X., 18F, 64Cu, and 68Ga Labeled RGD-Bombesin Heterodimeric Peptides for PET Imaging of Breast Cancer. *Bioconjugate Chem.* **2009,** *20*, 1016-1025.
35. Li, Z.-B.; Chen, K.; Chen, X., 68Ga-labeled multimeric RGD peptides for microPET imaging of integrin αvβ3 expression. *Eur. J. Nucl. Med. Mol. Imaging* **2008,** *35*, 1100-1108.
36. Velikyan, I.; Maecke, H.; Langstrom, B., Convenient Preparation of 68Ga-Based PET-Radiopharmaceuticals at Room Temperature. *Bioconjugate Chem.* **2008,** *19*, 569-573.
37. Jeong, J. M.; Hong, M. K.; Chang, Y. S.; Lee, Y.-S.; Kim, Y. J.; Cheon, G. J.; Lee, D. S.; Chung, J.-K.; Lee, M. C., Preparation of a Promising Angiogenesis PET Imaging Agent: 68Ga-Labeled c(RGDyK)–Isothiocyanatobenzyl-1,4,7-Triazacyclononane-1,4,7-Triacetic Acid and Feasibility Studies in Mice. *J. Nucl. Med.* **2008,** *49*, 830-836.
38. Notni, J.; Hermann, P.; Havlickova, J.; Kotek, J.; Kubicek, V.; Plutnar, J.; Loktionova, N.; Riss, P. J.; Rosch, F.; Lukes, I., A triazacyclononane-based bifunctional phosphinate ligand for the preparation of multimeric 68Ga tracers for positron emission tomography. *Chem. Eur. J.* **2010,** *16*, 7174-7185.
39. Notni, J.; Šimeček, J.; Hermann, P.; Wester, H.-J., TRAP, a Powerful and Versatile Framework for Gallium-68 Radiopharmaceuticals. *Chem. Eur. J.* **2011,** *17*, 14718-14722.
40. Notni, J.; Pohle, K.; Wester, H. J., Be spoilt for choice with radiolabelled RGD peptides: preclinical evaluation of (6)(8)Ga-TRAP(RGD)(3). *Nucl. Med. Biol.* **2013,** *40*, 33-41.
41. Ferreira, C. L.; Lamsa, E.; Woods, M.; Duan, Y.; Fernando, P.; Bensimon, C.; Kordos, M.; Guenther, K.; Jurek, P.; Kiefer, G. E., Evaluation of bifunctional chelates for the development of gallium-based radiopharmaceuticals. *Bioconjug Chem* **2010,** *21*, 531-536.
42. Tircsó, G.; Benyó, E. T.; Suh, E. H.; Jurek, P.; Kiefer, G. E.; Sherry, A. D.; Kovács, Z., (S)-5-(p-Nitrobenzyl)-PCTA, a Promising Bifunctional Ligand with Advantageous Metal Ion Complexation Kinetics. *Bioconjugate Chem.* **2009,** *20*, 565-575.
43. Ferreira, C. L.; Lamsa, E.; Woods, M.; Duan, Y.; Fernando, P.; Bensimon, C.; Kordos, M.; Guenther, K.; Jurek, P.; Kiefer, G. E., Evaluation of Bifunctional Chelates for the Development of Gallium-Based Radiopharmaceuticals. *Bioconjugate Chem.* **2010,** *21*, 531-536.
44. Ferreira, C. L.; Yapp, D. T. T.; Mandel, D.; Gill, R. K.; Boros, E.; Wong, M. Q.; Jurek, P.; Kiefer, G. E., 68Ga Small Peptide Imaging: Comparison of NOTA and PCTA. *Bioconjugate Chem.* **2012,** *23*, 2239-2246.
45. Gotzmann, C.; Braun, F.; Bartholoma, M. D., Synthesis, 64Cu-labeling and PET imaging of 1,4,7-triazacyclononane derived chelators with pendant azaheterocyclic arms. *RSC Advances* **2016,** *6*, 119-131.

46. Alhokbany, N. S. M.; Siddiqui, M. R. H.; Mahfouz, R. M., Synthesis, characterisation, DFT and biomedical investigation of new Ga(III) complex with imidazole. *J Chem Res* **2008**, 163-166.
47. Kratz, F.; Nuber, B.; Weiss, J.; Keppler, B. K., Synthesis and Characterization of Potential Antitumor and Antiviral Gallium(Iii) Complexes of N-Heterocycles. *Polyhedron* **1992,** *11*, 487-498.
48. Zanzonico, P., Routine Quality Control of Clinical Nuclear Medicine Instrumentation: A Brief Review. *J. Nucl. Med.* **2008,** *49*, 1114-1131.
49. Gaussian 03W, R. B., M. J. Frisch, G. W. Trucks, H. B. Schlegel, G. E. Scuseria, ; M. A. Robb, J. R. C., J. A. Montgomery, Jr., T. Vreven, ; K. N. Kudin, J. C. B., J. M. Millam, S. S. Iyengar, J. Tomasi, ; V. Barone, B. M., M. Cossi, G. Scalmani, N. Rega, ; G. A. Petersson, H. N., M. Hada, M. Ehara, K. Toyota, ; R. Fukuda, J. H., M. Ishida, T. Nakajima, Y. Honda, O. Kitao, ; H. Nakai, M. K., X. Li, J. E. Knox, H. P. Hratchian, J. B. Cross, ; C. Adamo, J. J., R. Gomperts, R. E. Stratmann, O. Yazyev, ; A. J. Austin, R. C., C. Pomelli, J. W. Ochterski, P. Y. Ayala, ; K. Morokuma, G. A. V., P. Salvador, J. J. Dannenberg, ; V. G. Zakrzewski, S. D., A. D. Daniels, M. C. Strain, ; O. Farkas, D. K. M., A. D. Rabuck, K. Raghavachari, ; J. B. Foresman, J. V. O., Q. Cui, A. G. Baboul, S. Clifford, ; J. Cioslowski, B. B. S., G. Liu, A. Liashenko, P. Piskorz, ; I. Komaromi, R. L. M., D. J. Fox, T. Keith, M. A. Al-Laham, ; C. Y. Peng, A. N., M. Challacombe, P. M. W. Gill, ; B. Johnson, W. C., M. W. Wong, C. Gonzalez, and J. A. Pople, ; Gaussian, I., Pittsburgh PA, 2003., **2003**.
50. Becke, A. D., Density-functional exchange-energy approximation with correct asymptotic behavior. *Phys. Rev. A* **1988,** *38*, 3098-3100.
51. Lee, C.; Yang, W.; Parr, R. G., Development of the Colle-Salvetti correlation-energy formula into a functional of the electron density. *Phys. Rev. B* **1988,** *37*, 785-789.
52. Stephens, P. J.; Devlin, F. J.; Chabalowski, C. F.; Frisch, M. J., Ab Initio Calculation of Vibrational Absorption and Circular Dichroism Spectra Using Density Functional Force Fields. *J. Phys. Chem.* **1994,** *98*, 11623-11627.
53. Dunning, T. H. J.; Hay, P. J., Modern Theoretical Chemistry. *Ed. H. F. Schaefer III, Vol. 3 (Plenum, New York) 1-28.* **1976,** *3*, 1-28.
54. Hay, P. J.; Wadt, W. R., Ab initio effective core potentials for molecular calculations. Potentials for K to Au including the outermost core orbitals. *J. Chem. Phys.* **1985,** *82*, 299-310.
55. Hay, P. J.; Wadt, W. R., Ab initio effective core potentials for molecular calculations. Potentials for the transition metal atoms Sc to Hg. *J. Chem. Phys.* **1985,** *82*, 270-283.
56. Wadt, W. R.; Hay, P. J., Ab initio effective core potentials for molecular calculations. Potentials for main group elements Na to Bi. *J. Chem. Phys.* **1985,** *82*, 284-298.
57. Godbout, N.; Salahub, D. R.; Andzelm, J.; Wimmer, E., Optimization of Gaussian-type basis sets for local spin density functional calculations. Part I. Boron through neon, optimization technique and validation. *Can. J. Chem.* **1992,** *70*, 560-571.
58. Sosa, C.; Andzelm, J.; Elkin, B. C.; Wimmer, E.; Dobbs, K. D.; Dixon, D. A., A local density functional study of the structure and vibrational frequencies of molecular transition-metal compounds. *J. Phys. Chem.* **1992,** *96*, 6630-6636.
59. Lee, Y.-S.; Hodošček, M.; Chun, J.-H.; Pike, V. W., Conformational Structure and Energetics of 2-Methylphenyl(2′-methoxyphenyl)iodonium Chloride: Evidence for Solution Clusters. *Chem. Eur. J.* **2010,** *16*, 10418-10423.
60. Hall, R. J.; Davidson, M. M.; Burton, N. A.; Hillier, I. H., Combined Density Functional, Self-Consistent Reaction Field Model of Solvation. *J. Phys. Chem.* **1995,** *99*, 921-924.

61. Chen, J. L.; Noodleman, L.; Case, D. A.; Bashford, D., Incorporating Solvation Effects into Density Functional Electronic Structure Calculations. *J. Phys. Chem.* **1994,** *98*, 11059-11068.
62. Tomasi, J.; Mennucci, B.; Cammi, R., Quantum Mechanical Continuum Solvation Models. *Chem. Rev.* **2005,** *105(8)*, 2999-3094.
63. Holland, J. P.; Green, J. C.; Dilworth, J. R., Probing the mechanism of hypoxia selectivity of copper bis(thiosemicarbazonato) complexes: DFT calculation of redox potentials and absolute acidities in solution. *Dalton. Trans.* **2006**, 783-794.
64. Connolly, M. L., Solvent-accessible surfaces of proteins and nucleic acids. *Science* **1983,** *221*, 709-713.
65. Adamo, C.; Barone, V., Toward reliable adiabatic connection models free from adjustable parameters. *Chem. Phys. Lett.* **1997,** *274*, 242-250.
66. Wadas, T. J.; Wong, E. H.; Weisman, G. R.; Anderson, C. J., Coordinating radiometals of copper, gallium, indium, yttrium, and zirconium for PET and SPECT imaging of disease. *Chem. Rev.* **2010,** *110*, 2858-2902.
67. Moore, D. A.; Fanwick, P. E.; Welch, M. J., A Novel Hexachelating Amino Thiol Ligand and Its Complex with Gallium(Iii). *Inorg. Chem.* **1990,** *29*, 672-676.
68. Sun, Y.; Anderson, C. J.; Pajeau, T. S.; Reichert, D. E.; Hancock, R. D.; Motekaitis, R. J.; Martell, A. E.; Welch, M. J., Indium (III) and gallium (III) complexes of bis(aminoethanethiol) ligands with different denticities: stabilities, molecular modeling, and in vivo behavior. *J. Med. Chem.* **1996,** *39*, 458-470.
69. Sun, Y. Z.; Martell, A. E.; Motekaitis, R. J.; Welch, M. J., Synthesis and stabilities of the Ga(III) and In(III) chelates of a new diaminodithiol bifunctional ligand. *Tetrahedron* **1998,** *54*, 4203-4210.
70. Sundberg, R. J.; Martin, R. B., Interactions of Histidine and Other Imidazole Derivatives with Transition-Metal Ions in Chemical and Biological-Systems. *Chem. Rev.* **1974,** *74*, 471-517.
71. Horner, K. E.; Karadakov, P. B., Shielding in and around Oxazole, Imidazole, and Thiazole: How Does the Second Heteroatom Affect Aromaticity and Bonding? *J. Org. Chem.* **2015,** *80*, 7150-7157.
72. Pearson, R. G., Hard and Soft Acids and Bases. *J. Am. Chem. Soc.* **1963,** *85*, 3533-3539.
73. Abdel-Magid, A. F.; Carson, K. G.; Harris, B. D.; Maryanoff, C. A.; Shah, R. D., Reductive Amination of Aldehydes and Ketones with Sodium Triacetoxyborohydride. Studies on Direct and Indirect Reductive Amination Procedures(1). *J. Org. Chem.* **1996,** *61*, 3849-3862.
74. Velikyan, I.; Maecke, H.; Langstrom, B., Convenient preparation of 68Ga-based PET-radiopharmaceuticals at room temperature. *Bioconjug. Chem.* **2008,** *19*, 569-573.
75. Mueller, D.; Klette, I.; Baum, R. P.; Gottschaldt, M.; Schultz, M. K.; Breeman, W. A. P., Simplified NaCl Based 68Ga Concentration and Labeling Procedure for Rapid Synthesis of 68Ga Radiopharmaceuticals in High Radiochemical Purity. *Bioconjugate Chem.* **2012,** *23*, 1712-1717.
76. Broan, C. J.; Cox, J. P. L.; Craig, A. S.; Kataky, R.; Parker, D.; Harrison, A.; Randall, A. M.; Ferguson, G., Structure and Solution Stability of Indium and Gallium Complexes of 1,4,7-Triazacyclononanetriacetate and of Yttrium Complexes of 1,4,7,10-Tetraazacyclododecanetetraacetate and Related Ligands - Kinetically Stable Complexes for Use in Imaging and Radioimmunotherapy - X-Ray Molecular-Structure of the Indium and Gallium Complexes of 1,4,7-Triazacyclononane-1,4,7-Triacetic Acid. *J. Chem. Soc. Perk. Trans. 2* **1991**, 87-99.

77. Prata, M. I.; Santos, A. C.; Geraldes, C. F.; de Lima, J. J., Structural and in vivo studies of metal chelates of Ga(III) relevant to biomedical imaging. *J. Inorg. Biochem.* **2000,** *79*, 359-363.
78. Goggin, P. L.; Buick, T. G., Distortion of Tetrachlorogallate Ion in Solution. *Chem. Commun.* **1967**, 290-291.
79. Bhalla, R.; Levason, W.; Luthra, S. K.; McRobbie, G.; Sanderson, G.; Reid, G., Radiofluorination of a pre-formed gallium(III) aza-macrocyclic complex: towards next-generation positron emission tomography (PET) imaging agents. *Chem. Eur. J.* **2015,** *21*, 4688-4694.
80. Malathi, M.; Sabesan, R.; Krishnan, S., IR carbonyl band intensity studies in N,N-dimethyl formamide and N,N-dimethyl acetamide on complex formation with phenols. *Curr. Sci.* **2004,** *86*, 838-842.
81. King, S. T., Low-Temperature Matrix Isolation Study of Hydrogen-Bonded, High-Boiling Organic Compounds .3. Infrared-Spectra of Monomeric Acetamide, Urea and Urea-D. *Spectrochim Acta a-M* **1972,** *A 28*, 165-&.
82. Suzuki, I., Infrared Spectra and Normal Vibrations of Acetamide and Its Deuterated Analogues. *Bull. Chem. Soc. Jpn.* **1962,** *35*, 1279-1286.

Figure and Scheme Legends

Scheme 1. Common ligands for ^{68}Ga chelation

Scheme 2. Novel TACN derived chelators of this work bearing five-membered azaheterocyclic arms

Scheme 3. Syntheses of the BFC NODIA-Me **4**, model compound **5** and PSMA targeting conjugate **7**. i) glyoxylic acid, $NaBH(OAc)_3$, DCE; ii) methylamine, HATU, DIPEA, DMF; iii) Glu-CO-Lys(Ahx)-$(tBu)_3$ ester, HATU, DIPEA, DMF; iv) 5M HCl, r.t.

Figure 1. Radiochemical conversion of ligands NOTI-Me **1**, NOTThia **2** and NOTA in ^{68}Ga labelling experiments in 0.2 M sodium acetate pH 4.0

Figure 2. Proton NMR spectra of (A) NOTI-Me **1**, (B) Ga-**1**, (C) NODIA-Me-NH-Me **5** and Ga-**5**

Figure 3. Representative radio-HPLC chromatograms of ^{68}Ga-**7** showing formation of newly formed species after incubation in different media. (A) saline (product formulation) after 4 h, (B) 50 mM DTPA pH 7.4 after 4 h, and human serum after 1 h and 4 h (C, D).

Figure 4. (A) Plot of the absolute concentration (nM) of daughter peak ^{68}Ga(OH)-**7** (9.20 min.) vs. time for two different initial concentrations of the ^{68}Ga complex. (B) Plot of the relative

percentage change (%) in the activity associated with the daughter peak ^{68}Ga(OH)-**7** with respect to that of the parent complex ^{68}Ga(Cl)-**7** vs. time. (C) Plot of the relative percentage change (%) in the activity associated with the daughter peak with respect to that of the parent complex vs. time at varying pH values (0.1M HEPES buffer) and in the control medium (water, pH 5.5). (D) Plot of the observed rate constants (log k_{obs}) versus log[OH^-] showing a linear relationship with a slope equal to the order of reaction with respect to the concentration of hydroxide anions.

Figure 5. (A) Representative maximum intensity projection of the biodistribution of ^{68}Ga-**7** in healthy nude mice at different time points. (B) Corresponding time-activity curves for organs of interest

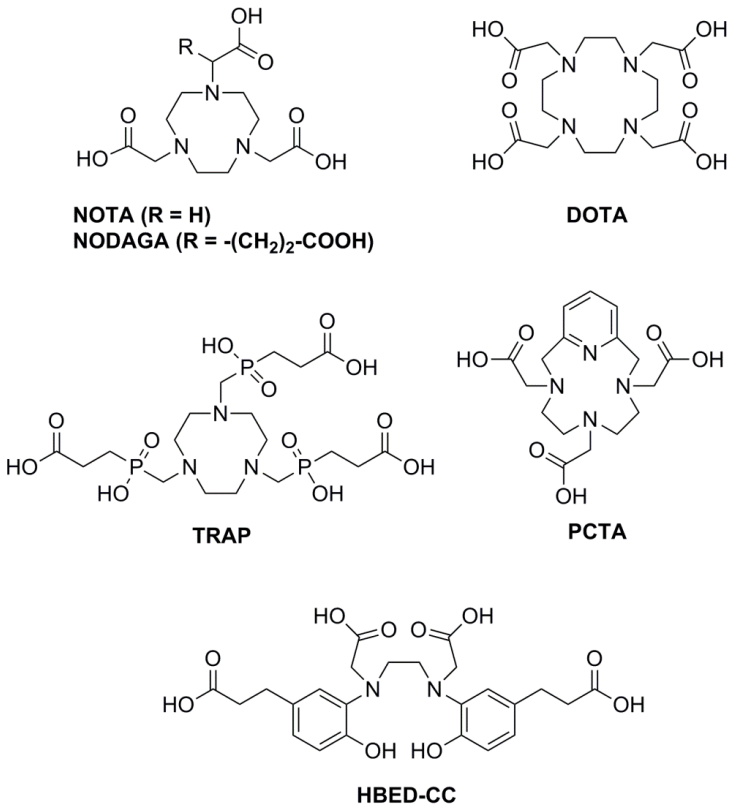

Scheme 1.

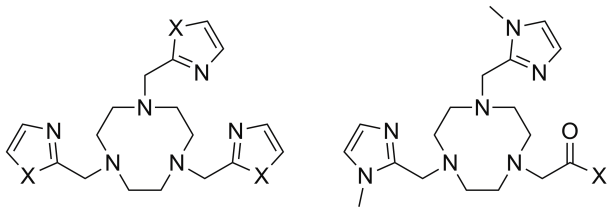

NOTI-Me **1** (X = N-Me)
NOTThia **2** (X = S)

NODIA-Me **4** (X = OH)
NODIA-Me-NH-Me **5** (X = NH-Me)

Scheme 2.

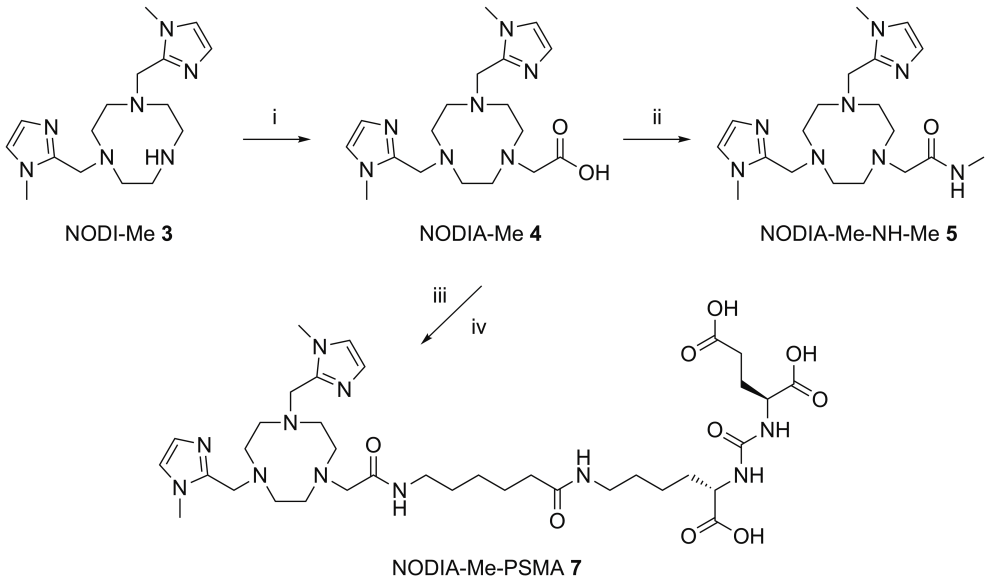

NODI-Me **3**

NODIA-Me **4**

NODIA-Me-NH-Me **5**

NODIA-Me-PSMA **7**

Scheme 3.

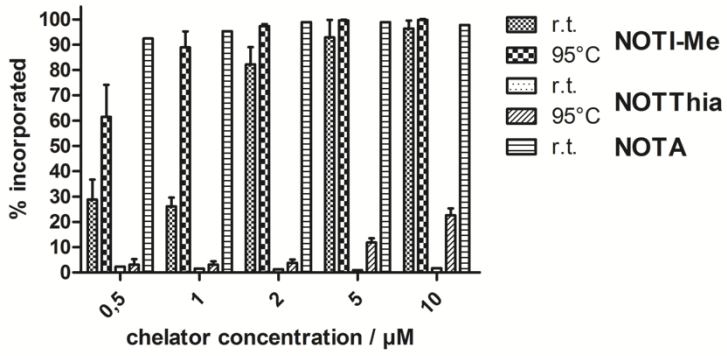
% incorporated
100
90
80
70
60
50
40
30
20
10
0
0,5
1
2
5
10
chelator concentration / µM
r.t.
95°C
NOTI-Me
r.t.
95°C
NOTThia
r.t.
NOTA

Figure 1.

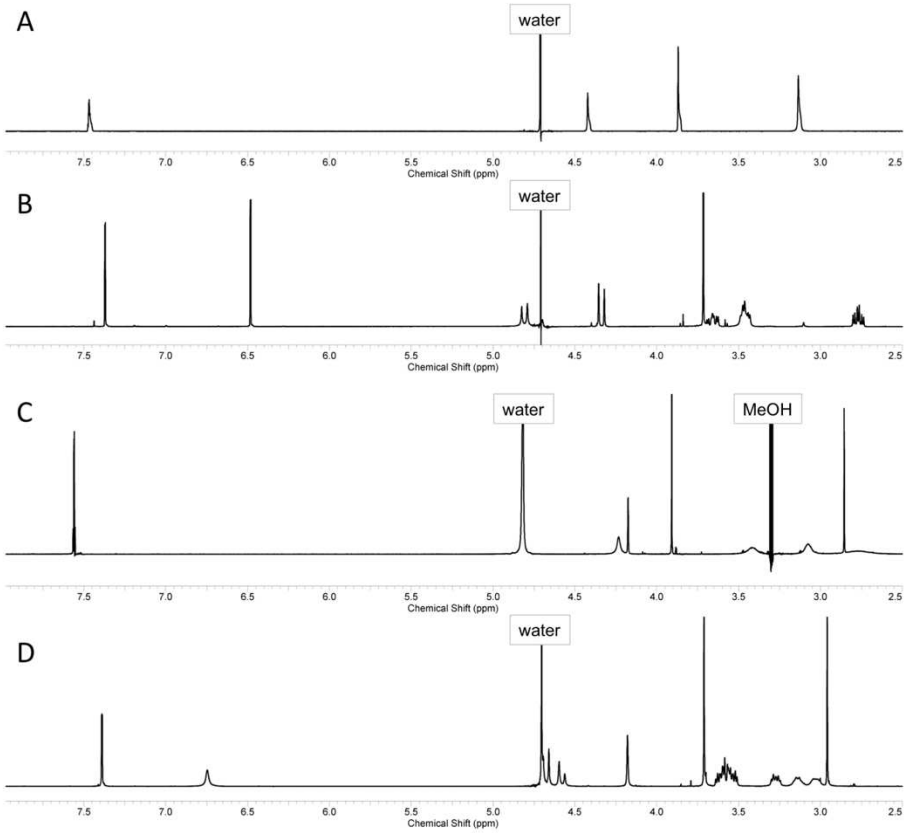
A
water
7.5
7.0
6.5
6.0
5.5
5.0
4.5
4.0
3.5
3.0
2.5
Chemical Shift (ppm)
B
water
7.5
7.0
6.5
6.0
5.5
5.0
4.5
4.0
3.5
3.0
2.5
Chemical Shift (ppm)
C
water
MeOH
7.5
7.0
6.5
6.0
5.5
5.0
4.5
4.0
3.5
3.0
2.5
Chemical Shift (ppm)
D
water
7.5
7.0
6.5
6.0
5.5
5.0
4.5
4.0
3.5
3.0
2.5
Chemical Shift (ppm)

Figure 2.

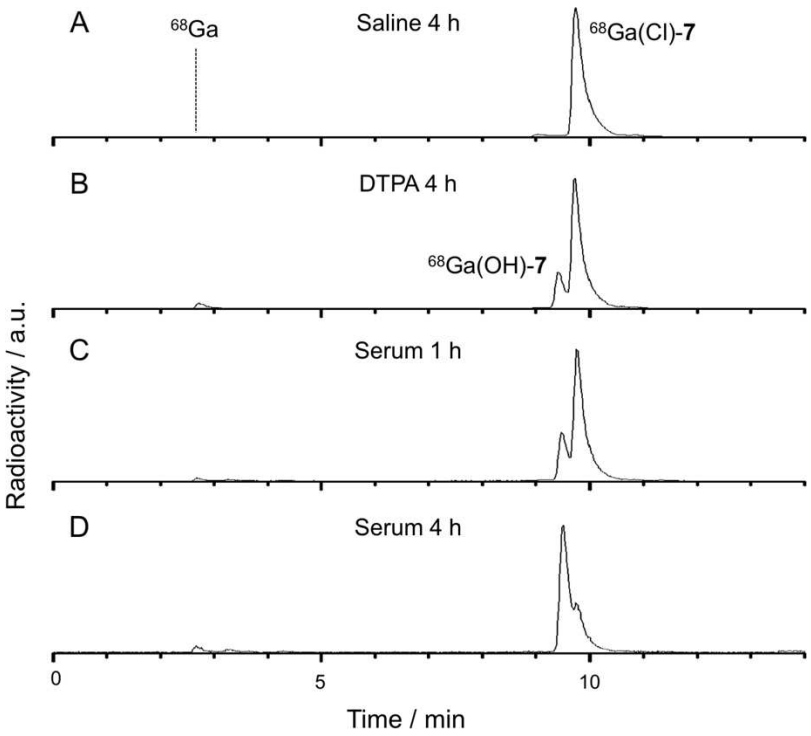
A
^{68}Ga
Saline 4 h
^{68}Ga(Cl)-7
B
DTPA 4 h
^{68}Ga(OH)-7
C
Serum 1 h
D
Serum 4 h
Radioactivity / a.u.
0
5
10
Time / min

Figure 3.

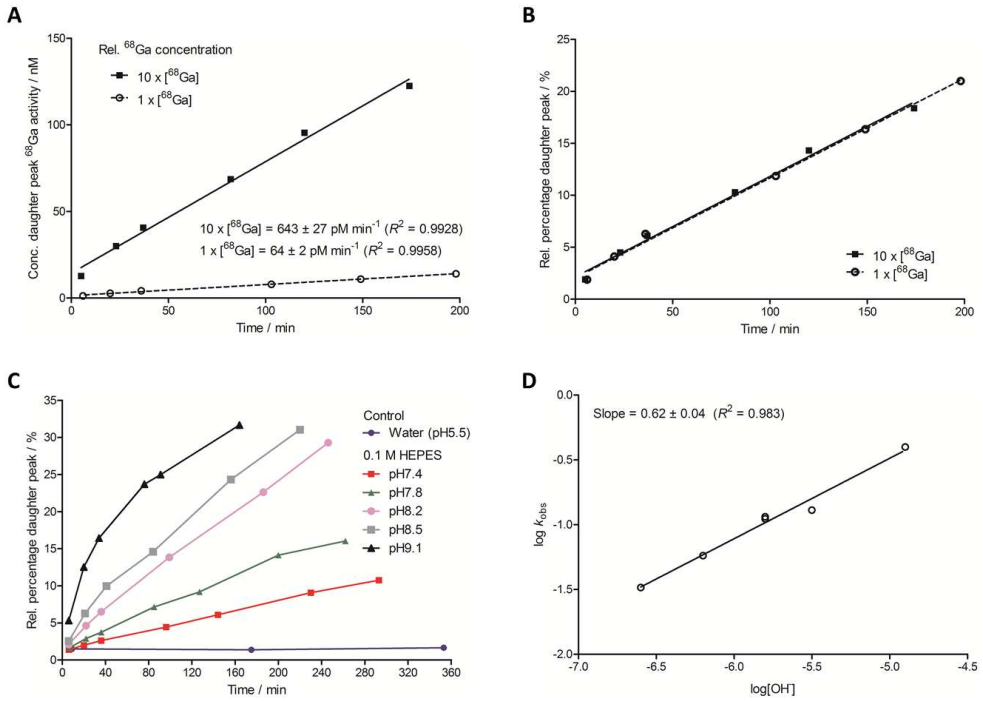
A
Rel. 68Ga concentration
10 x [68Ga]
1 x [68Ga]
Conc. daughter peak 68Ga activity / nM
10 x [68Ga] = 643 ± 27 pM min-1 (R2 = 0.9928)
1 x [68Ga] = 64 ± 2 pM min-1 (R2 = 0.9958)
Time / min
B
Rel. percentage daughter peak / %
10 x [68Ga]
1 x [68Ga]
Time / min
C
Rel. percentage daughter peak / %
Control
Water (pH5.5)
0.1 M HEPES
pH7.4
pH7.8
pH8.2
pH8.5
pH9.1
Time / min
D
Slope = 0.62 ± 0.04 (R2 = 0.983)
log kobs
log[OH-]

Figure 4.

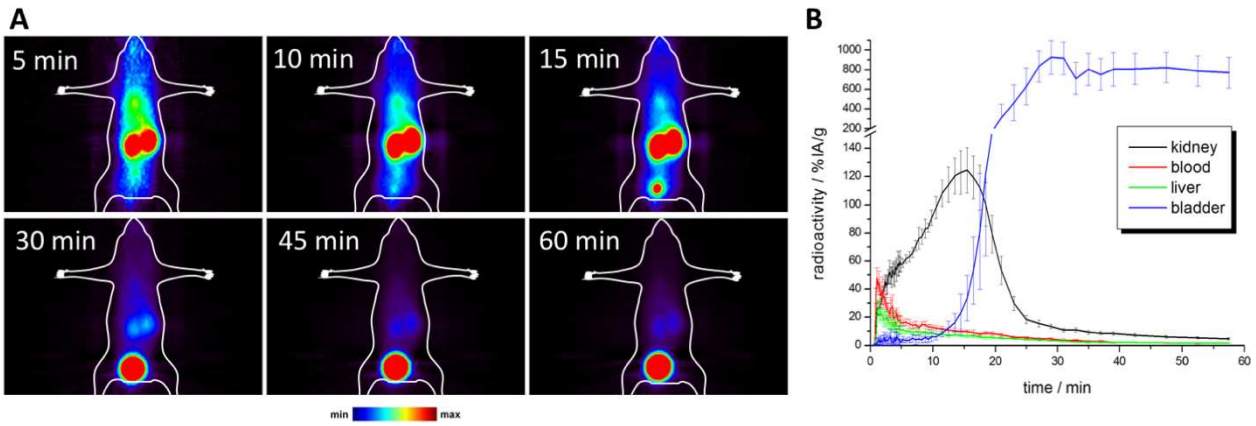
A
5 min
10 min
15 min
30 min
45 min
60 min
min
max
B
radioactivity / %IA/g
time / min
kidney
blood
liver
bladder

Figure 5.

For table of contents only

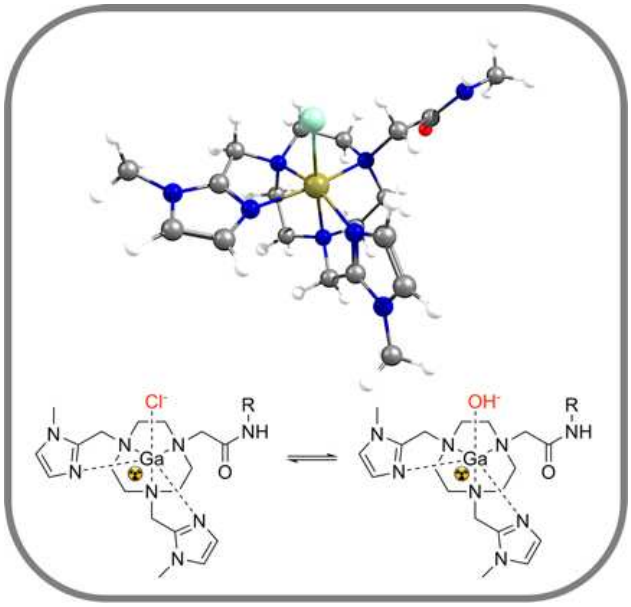

We recently demonstrated the applicability of 1,4,7-triazacyclononane derived ligands with up to three azaheterocyclic arms as chelating agents for ^{64}Cu used in Positron Emission Tomography (PET). Here, we describe their complex formation with the PET isotope $^{68}Ga^{3+}$. These ligands form rigid 1:1 chelates with $^{nat}Ga^{3+}$ in solution. In $^{68}Ga^{3+}$ complexes of the five-coordinate bifunctional chelator NODIA-Me, the remaining coordination site of the octahedron is occupied by monodentate ligands such as chloride or hydroxide.